January 4, 2008
Mark T EricksonKirk, mtk@nrc.gov, markericksonkirk@verizon.net
Do not further distribute

Appendix G

Further Evaluation of High Fluence Data

Draft of January 4, 2008

Contents

Contents....2
Tables....3
Figures....3
1 Introduction....6
2 Data Collection and Assessment Procedure....7
3 High-fluence Database and its Comparison to the Embrittlement Trend Curves Developed in the Main Body of this Report....9
4 Summary and Recommendations....17
5 References....18

Tables

Table G.1. Summary of citations used in the high fluence data review. 10
Table G.2. Summary materials and irradiation condition studied in CRP-1. 21
Table G.3. Summary materials and irradiation condition studied in CRP-2. 23
Table G.4. Summary materials and irradiation condition studied in CRP-3. 25
Table G.5. Summary materials and irradiation condition studied in Hawthorne 85. 34
Table G.6. Summary materials and irradiation condition studied in Fabry 96. 36
Table G.7. Summary materials and irradiation condition studied in Kussmaul 90. 38
Table G.8. Summary materials and irradiation condition studied in Brillaud 01. 40
Table G.9. Summary materials and irradiation condition studied in Bellman 90. 43
Table G.10. Summary materials and irradiation condition studied in Ishino 90. 45
Table G.11. Summary materials and irradiation condition studied in Pachur 93. 47
Table G.12. Summary materials and irradiation condition studied in Leitz 93. 49
Table G.13. Summary materials and irradiation condition studied in Onizawa 01. 51
Table G.14. Summary materials and irradiation condition studied in Lee 01. 53
Table G.15. Summary materials and irradiation condition studied in Nanstad 04. 55
Table G.16. Summary materials and irradiation condition studied in Gérard 06. 57
Table G.17. Summary materials and irradiation condition studied in RADAMO 05. 59
Table G.18. Summary materials and irradiation condition studied in JNES 07 61

Figures

Figure G-1. Distribution of fluences in the US LWR Database. 6
Figure G-2. Distribution of chemical composition in the high-fluence database taken from the literature. 12
Figure G-3. Distribution of neutron flux in the high-fluence database taken from the literature. 13
Figure G-4. Assessment of how well plates in the high-fluence database are predicted by (top) the ΔT_{30} model RM-6(2), which was calibrated only to US-LWR surveillance data, and by (bottom) the ΔT_{30} model recommended for use in Revision 3 of Regulatory Guide 1.99. The horizontal lines indicate $\pm 2\sigma$ confidence bounds, and the brown circles indicate two shift value having high nickel content. 14
Figure G-5. Assessment of how well forgings in the high-fluence database are predicted by (top) the ΔT_{30} model RM-6(2), which was calibrated only to US-LWR surveillance data, and by (bottom) the ΔT_{30} model recommended for use in Revision 3 of Regulatory Guide 1.99. The horizontal lines indicate $\pm 2\sigma$ confidence bounds. 15
Figure G-6. Assessment of how well plates in the high-fluence database are predicted by (top) the ΔT_{30} model RM-6(2), which was calibrated only to US-LWR surveillance data, and by (bottom) the ΔT_{30} model recommended for use in Revision 3 of Regulatory Guide 1.99. The horizontal lines indicate $\pm 2\sigma$ confidence bounds, and the brown circles/ovals indicate shift values having high nickel content. 16

Figure G-7. Assessment of how well CRP-1 data are predicted by (top) the ΔT_{30} model RM-6(2), which was calibrated only to US-LWR surveillance data, and by (bottom) the ΔT_{30} model recommended for use in Revision 3 of Regulatory Guide 1.99. 22
Figure G-8. Assessment of how well CRP-2 data are predicted by (top) the ΔT_{30} model RM-6(2), which was calibrated only to US-LWR surveillance data, and by (bottom) the ΔT_{30} model recommended for use in Revision 3 of Regulatory Guide 1.99. 24
Figure G-9. Assessment of the effect of assumed flux on now well CRP-3 data are predicted by the ΔT_{30} model RM-6(2). In the top, middle, and bottom graphs the assumed flux was set equal to $1x10^{12}$, $1x10^{13}$, and $1x10^{14}$ n/cm^2/s, respectively..... 26
Figure G-10. Assessment of how well CRP-3 data are predicted by (top) the ΔT_{30} model RM-6(2), which was calibrated only to US-LWR surveillance data, and by (bottom) the ΔT_{30} model recommended for use in Revision 3 of Regulatory Guide 1.99. Assumed flux was $1x10^{13}$ n/cm^2/s. 27
Figure G-11. Range of neutron flux values in TR-EDB. 28
Figure G-12. Range of copper, nickel, and phosphorus contents in TR-EDB. 29
Figure G-13. Assessment of how well data from the TR-EDB database are predicted by (top) the ΔT_{30} model RM-6(2), which was calibrated only to US-LWR surveillance data, and by (bottom) the ΔT_{30} model recommended for use in Revision 3 of Regulatory Guide 1.99. Plots show the full nickel range in TR-EDB; division between low and high flux is made at 10^{12} n/cm^2/s. 30
Figure G-14. Assessment of how well data from the TR-EDB database are predicted by (top) the ΔT_{30} model RM-6(2), which was calibrated only to US-LWR surveillance data, and by (bottom) the ΔT_{30} model recommended for use in Revision 3 of Regulatory Guide 1.99. In this figure nickel is limited to 1.25 wt-%; division between low and high flux is made at 10^{12} n/cm^2/s. 31
Figure G-15. Assessment of how well data from the TR-EDB database are predicted by (top) the ΔT_{30} model RM-6(2), which was calibrated only to US-LWR surveillance data, and by (bottom) the ΔT_{30} model recommended for use in Revision 3 of Regulatory Guide 1.99. Plots show the full nickel range in TR-EDB; division between low and high flux is made at 10^{12} n/cm^2/s. 32
Figure G-16. Assessment of how well data from the TR-EDB database are predicted by (top) the ΔT_{30} model RM-6(2), which was calibrated only to US-LWR surveillance data, and by (bottom) the ΔT_{30} model recommended for use in Revision 3 of Regulatory Guide 1.99. In this figure nickel is limited to 1.25 wt-%; division between low and high flux is made at 10^{12} n/cm^2/s. 33
Figure G-17. Assessment of how well Hawthorne 85 data are predicted by (top) the ΔT_{30} model RM-6(2), which was calibrated only to US-LWR surveillance data, and by (bottom) the ΔT_{30} model recommended for use in Revision 3 of Regulatory Guide 1.99. 35
Figure G-18. Assessment of how well Fabry 96 data are predicted by (top) the ΔT_{30} model RM-6(2), which was calibrated only to US-LWR surveillance data, and by (bottom) the ΔT_{30} model recommended for use in Revision 3 of Regulatory Guide 1.99. 37
Figure G-19. Comparison of fluence and flux conditions reported by Kussmaul with the larger data sets documented in the main body of this report..... 38
Figure G-20. Assessment of how well Kussmaul 90 data are predicted by (top) the ΔT_{30} model RM-6(2), which was calibrated only to US-LWR surveillance data, and by (bottom) the ΔT_{30} model recommended for use in Revision 3 of Regulatory Guide 1.99. 39
Figure G-21. Assessment of how well Brillaud 01 data are predicted by (top) the ΔT_{30} model RM-6(2), which was calibrated only to US-LWR surveillance data, and by (bottom) the ΔT_{30} model recommended for use in Revision 3 of Regulatory Guide 1.99. 41

Figure G-22. Assessment of how well Brillaud 92 data for the overall French RPV surveillance program are predicted by (top) the ΔT_{30} model RM-6(2), which was calibrated only to US-LWR surveillance data, and by (bottom) the ΔT_{30} model recommended for use in Revision 3 of Regulatory Guide 1.99. The low temperature data shown in these plots are a subset of the Chooz-A data reported in Brillaud 01. 42
Figure G-23. Assessment of how well Bellman 90 data are predicted by (top) the ΔT_{30} model RM-6(2), which was calibrated only to US-LWR surveillance data, and by (bottom) the ΔT_{30} model recommended for use in Revision 3 of Regulatory Guide 1.99. 44
Figure G-24. Assessment of how well Ishino 90 data are predicted by (top) the ΔT_{30} model RM-6(2), which was calibrated only to US-LWR surveillance data, and by (bottom) the ΔT_{30} model recommended for use in Revision 3 of Regulatory Guide 1.99. 46
Figure G-25. Assessment of how well Pachur 93 data are predicted by (top) the ΔT_{30} model RM-6(2), which was calibrated only to US-LWR surveillance data, and by (bottom) the ΔT_{30} model recommended for use in Revision 3 of Regulatory Guide 1.99. 48
Figure G-26. Assessment of how well Leitz 93 data are predicted by (top) the ΔT_{30} model RM-6(2), which was calibrated only to US-LWR surveillance data, and by (bottom) the ΔT_{30} model recommended for use in Revision 3 of Regulatory Guide 1.99. 50
Figure G-27. Assessment of how well Onizawa 01 data are predicted by (top) the ΔT_{30} model RM-6(2), which was calibrated only to US-LWR surveillance data, and by (bottom) the ΔT_{30} model recommended for use in Revision 3 of Regulatory Guide 1.99. 52
Figure G-28. Assessment of how well Lee 01 data are predicted by (top) the ΔT_{30} model RM-6(2), which was calibrated only to US-LWR surveillance data, and by (bottom) the ΔT_{30} model recommended for use in Revision 3 of Regulatory Guide 1.99. 54
Figure G-29. Assessment of how well Nanstad 04 data are predicted by (top) the ΔT_{30} model RM-6(2), which was calibrated only to US-LWR surveillance data, and by (bottom) the ΔT_{30} model recommended for use in Revision 3 of Regulatory Guide 1.99. 56
Figure G-30. Assessment of how well Gérard 06 data are predicted by (top) the ΔT_{30} model RM-6(2), which was calibrated only to US-LWR surveillance data, and by (bottom) the ΔT_{30} model recommended for use in Revision 3 of Regulatory Guide 1.99. 58
Figure G-31. Assessment of how well RADAMO 05 data are predicted by (top) the ΔT_{30} model RM-6(2), which was calibrated only to US-LWR surveillance data, and by (bottom) the ΔT_{30} model recommended for use in Revision 3 of Regulatory Guide 1.99. 60
Figure G-32. Distribution of copper and nickel in the JNES databases. 61
Figure G-33. Assessment of how well JNES 07 data are predicted by (top) the ΔT_{30} model RM-6(2), which was calibrated only to US-LWR surveillance data, and by (bottom) the ΔT_{30} model recommended for use in Revision 3 of Regulatory Guide 1.99. 62

1 Introduction

One of the major findings from the main body of this report was the need to modify the ΔT_{30} ETC that was calibrated to the USLWR surveillance database to take account of embrittlement observed at fluences that, while relevant in the period of license extension, lie beyond the bulk of the surveillance database. As shown in Figure G-1, less than 10% of the USLWR surveillance data was obtained at fluences above $3x10^{19}$ n/cm^2. Nevertheless, during the period of first and second license extension, and for new reactors, the prediction of embrittlement trends to fluences as high as $\approx 1x10^{20}$ n/cm^2 will be critical to ensuring the continued operating integrity of RPV structures.

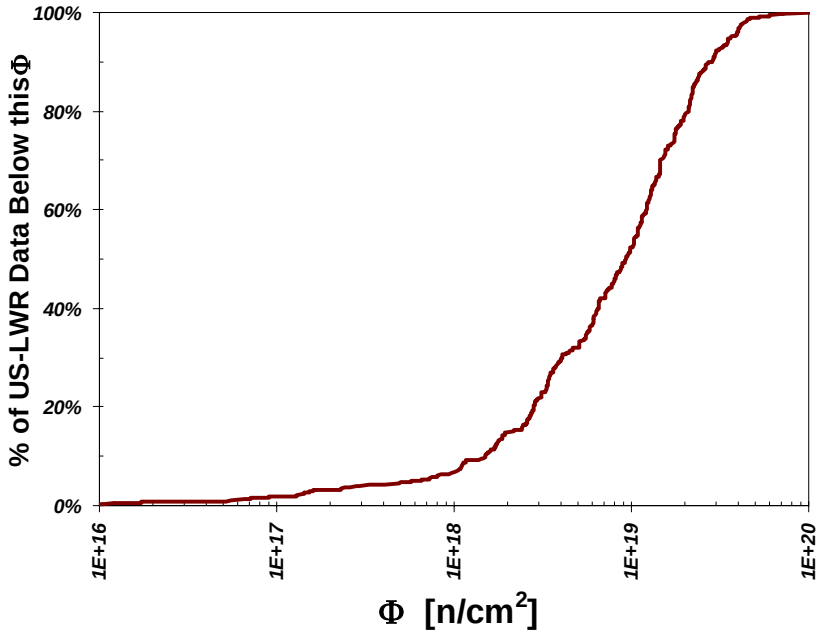

Figure G-1. Distribution of fluences in the US LWR Database.

The main body of this report included an assessment of the prediction accuracy at high fluences of RM-6(2), a ΔT_{30} ETC calibrated to the USLWR surveillance data. In comparison with test reactor data obtained by Chaouadi [Chaouadi 05] and by JNES [JNES 07], the RM-6(2) predictions of ΔT_{30} were invariably low (underestimates) for fluences above $\approx 3x10^{19}$ n/cm^2 (see Figures 4-39 and 4-42 in the main text) despite the fact that RM-6(2) provided good predictions of lower fluence data from these same data sets. These test reactor data were viewed as being relevant to the prediction of embrittlement trends in commercial power reactors despite the high fluxes at which the data were obtained because of two data sets reported by Gérard [Gérard 06]. Gérard obtained data from both test and power reactors to fluences as high as $\approx 1x10^{20}$ n/cm^2. Despite an approximately 500-fold increase in the flux between the power reactor irradiations ($1.3\text{-}1.5x10^{11}$ n/cm^2/s) and the test reactor irradiations ($5\text{-}9x10^{13}$ n/cm^2/s) Gérard's two data sets (see Figure 4-32 in the main text) show no significant effect of flux on ΔT_{30} embrittlement trends. The Gérard data thus suggest that the ΔT_{30} ETCs calibrated to the USLWR surveillance data will non-conservatively predict the effect of embrittlement at high fluences for fluxes characteristic of ***both*** power and test reactors, with the degree of non-conservatism increasing as the level of neutron fluence increases.

In an effort to obtain the best informed predictions of high fluence embrittlement trends that are possible within the current state of knowledge, a review of the literature was conducted to obtain a more comprehensive empirical basis to inform our treatment of the high fluence regime. This review, which is reported in Sections 2 and 3, revealed not only significant amounts of test reactor data but also some power reactor data. The aim of this review was to provide insight regarding the following two questions:

- Are the embrittlement trends revealed by the RADAMO and JNES test reactor databases at high fluences consistent with other test reactor data that have previously been reported in the literature?
- Is there a significant effect of flux on the total embrittlement magnitude that occurs at high fluences such that the trends exhibited by test reactor data (high flux) differ significantly from the trends exhibited by power reactor data (low flux)?

The information obtained by these activities provides the basis for our recommended procedure for predicting ΔT_{30} in the high fluence regime, which appears in Section 4

2 Data Collection and Assessment Procedure

In this review we have restricted attention to studies that obtained data at high fluences. If a data set was found in the literature having measured values of ΔT_{30} or ΔYS at fluences above $3x10^{19}$ n/cm^2 then the entire data set was retained for analysis. Conversely, data sets restricted to fluences below $3x10^{19}$ n/cm^2 were excluded from this analysis. Additionally, to ensure the relevance of the data analyzed to LWRs operating in the United States, and to minimize uncertainties to the greatest extent possible, the scope of the literature review was restricted, as follows:

- Steels that are not typical of US RPV construction (e.g., Magnox steels, VVER steels) were excluded.
- Low temperature irradiations (e.g., the close to ambient temperature irradiation received by the High Flux Isotope Reactor (HFIR) at Oak Ridge) were excluded.
- Measurements performed on sub-size and/or precracked Charpy specimens were excluded.

These restrictions were applied uniformly, with the exception of the second restriction on temperature. As detailed in Annex 1, the restriction on temperature was waived in one instance to enable examination of data from the French power reactor Chooz-A, which operated at 491 °F from 1967-1975, then at 509 °F from 1975-1991.

Data from the literature were considered, as follows:

1. With the exception of data collected under Item 2 below, data from before (approximately) 1990 was assumed to be summarized in the *Test Reactor Embrittlement Data Base*, or TR-EDB, which was compiled by the Oak Ridge National Laboratory under contract to the NRC and is reported in NUREG/CR-6076 [Stallmann 94].
2. From 1974 through the present day the International Atomic Energy Agency (IAEA) has conducted a series of Cooperative Research Projects (CRPs) aimed at understanding and quantifying the effects of irradiation damage on the mechanical properties (strength, Charpy impact, fracture toughness, hardness) of RPV steels. Data from reports and databases compiled as part of these projects were considered as part of our review.

3. A survey of the literature since (approximately) 1990 was conducted to obtain any other high fluence information that has been reported.

Table G.1 summarizes the various data sources from which high fluence data have been obtained. For completeness data that were already presented in the main text are repeated in this table; these data will also be analyzed in a manner consistent with the literature data in this Appendix. All data taken from the citations listed in Table G.1 are compared here to the trend curves developed in the main body of this document; the comparison for each data set is structured as follows:

- First the data from the citation is identified as falling into one of the following three categories:
  - Only high flux / test reactor data
  - Only low flux / power reactor data
  - Both high and low flux data (i.e., both test and power reactor irradiations)
- Second the source of the data, material, test, and irradiation conditions are described briefly, making use of a consistent tabular format. In situations where assumptions had to be made to enable comparison of the published data with the predictions of a trend curve these assumptions are called out and explained.
- Third the data are compared with trend curve RM-6(2), which was developed by fitting only the ΔT_{30} data in the US LWR surveillance database. In situations where only ΔYS data are available for comparison, the ΔYS values (which have units of MPa) are converted to ΔT_{30} values (which have units of °F) using the following formula, which appeared as Eq. 4-19 in the main text:

$$\Delta T_{30} = \left\{ \begin{array}{l} Weld = 1.39 \\ Plate = 1.18 \\ Forging = 0.84 \end{array} \right\} \cdot \Delta YS$$

  Based on the information presented in the main text the expectation is that the measured ΔT_{30} values will compare favorably with the predictions of RM-6(2) at fluences below $\approx 3 \times 10^{19}$ n/cm^2, but that RM-6(2) will begin to under-predict measured ΔT_{30} values as fluence increases above this value.
- Finally the data are compared with trend curve that was recommended in the main text for adoption in Revision 3 or Regulatory Guide 1.99, which consists of RM-6(2) at low fluences and an ETC that was based on the RADAMO data at higher fluences (this equation is described in Section 4.5 of the main text). If only ΔYS data are available for comparison, the ΔYS values are converted to ΔT_{30} values using the procedure just described. Based on the information presented in the main text the expectation is that the measured ΔT_{30} values will compare favorably with the predictions of this equation at all fluences.

As revealed by Table G.1, this literature review has obtained over 1100 individual shift values. The data from each citation are assessed using the method just described in Annex 1 of this Appendix. Section 3 provides a description of the entire high-fluence database and a comparison of the data within it to the predictions of the embrittlement trend curves developed in the main body of this report. This assessment provides the basis for our recommended treatment of high fluence data in Revision 3 of Regulatory Guide, which are made in Section 4.

3 High-fluence Database and its Comparison to the Embrittlement Trend Curves Developed in the Main Body of this Report

Figure G-2 shows the distribution of chemical composition for the 1100+ ΔT_{30} and ΔYS values in the high-fluence database. The composition range revealed in these figures is broadly consistent with that exhibited by the USLWR surveillance database. Figure G-3 shows the distribution flux for the high-fluence database. While the bulk of these data were obtained in test reactor irradiations (fluxes above $1x10^{12}$ n/cm^2/s), 180 ΔT_{30} or ΔYS shift values (16% of the database) were obtained at the lower fluxes that are characteristic of power reactor operations.

The top graph on Figure G-4 provides an assessment of how well plates in the high-fluence database are predicted by the ΔT_{30} model RM-6(2), which was calibrated only to US-LWR surveillance data. Consistent with the information provided in the main body of this report, these data show that the RM-6(2) model provides a good representation of embrittlement trends at low fluences. However, RM-6(2) does not provide a good representation of embrittlement trends at fluences higher than those characteristic of the bulk of the US-LWR database. As noted in the main body of the text, as fluence increases beyond $\approx 3x10^{19}$ n/cm^2, RM-6(2) becomes progressively less accurate, systematically under-estimating the magnitude of embrittlement. Comparison of the low flux / power reactor data with the more numerous high flux / test reactor data reveals consistent trends between these two conditions. There is no effect of flux on embrittlement in these data that is significant enough to emerge from the background scatter that is characteristic of both the USLWR and the high-fluence databases. Plates having high nickel content are specifically called out on this diagram because it was noted in the main body of this report that RM-6(2) does not provide an accurate representation of embrittlement trends in high-nickel materials, irrespective of fluence.

The bottom graph on Figure G-4 provides an assessment of how well plates in the high-fluence database are predicted by the ΔT_{30} model that was recommended for use in Revision 3 of Regulatory Guide 1.99. Consistent with the information provided in the main body of this report, these data show that the high fluence correction that was incorporated into this model allows it to make accurate predictions of embrittlement trends across the entire spectrum of fluences contained in this database. As was the case when the data were compared with the RM-6(2) model, the trends shown by low flux / power reactor are consistent with the trends shown by the more numerous high flux / test reactor data.

Table G.1. Summary of citations used in the high fluence data review.

Short Identifier	Embrittlement Shift Metric		Reactor Type		Number of Shift Data	Full Citation
	ΔT_{30}	ΔYS	Power	Test		
CRP-1	X			X	16	IAEA-176, "Co-ordinated Research Programme on Irradiation Embrittlement of Pressure Vessel Steels," International Atomic Energy Agency, 1975.
CRP-2	X			X	79	TRS-265, "Analysis of the Behaviour of Advanced Reactor Pressure Vessel Steels under Neutron Irradiation," 1986.
CRP-3	X			X	49	Unpublished Report and Database: Optimizing of Reactor Pressure Vessel Surveillance Programmes and their Analyses
TR-EDB	X		X	X	263	E W. Stallmann, J. A. Wang, E B., and K. Kam, "TR-EDB: Test Reactor Embrittlement Data Base, Version 1," NUREG/CR-6076, United States Nuclear Regulatory Commission, 1994.
Hawthorne 85	X		X	X	11	Hawthorne, J.R., Menke, B.H., and Hiser, A.L., "Notch Ductility and Fracture Toughness Degradation of Pressure Vessel Steel Reference Plates from Pool Side Facility (PSF) Irradiation Capsules," *Effects of Radiation on Materials: 12th International Symposium, ASTM STP 870*, F.A. Garner and J.S. Perrin, Eds., American Society for Testing and Materials, Philadelphia, 1985, pp. 1163-1186.
Fabry 96	X		X	X	59	Fabry, A., et al., "Research to Understand the Embrittlement Behavior of Yankee/BR3 Surveillance Plate and Other Outlier RPV Steels," *Effects of Radiation on Materials: 17th International Symposium, ASTM STP 1270*, D.S. Gelles, R.K. Nanstad, A.S. Kumar, and E.A. Little, Eds., American Society for Testing and Materials, Philadelphia, 1996, pp. 138-187.
Kussmaul 90	X		X		8	Kussmaul, K., Föhl, J., and Weissenberg, T., "Investigation of Materials from a Decommissioned Reactor Pressure Vessel – A Contribution to the Understanding of Irradiation Embrittlement, *Effects of Radiation on Materials: 14th International Symposium, ASTM STP 1046*, N.H. Packin, R.E. Stoller, and A.S. Kumar, Eds., American Society for Testing and Materials, Philadelphia, 1990, pp. 80-104.
Brillaud 01	X		X		17	Brillaud, C., Grandjean, Y., and Saillet, S., "Vessel Investigation Program of 'CHOOZ A' PWR Reactor after Shutdown," *Effects of Radiation on Materials: 20th International Symposium, ASTM STP 1405*, S.T. Rosinski, M.L. Grossbeck, T.R. Allen, and A.S. Kumar, Eds., American Society for Testing and Materials, West Conshohcken Pennsylvania, 2001, pp. 28-41.
Bellmann 90	X			X	65	Bellmann, D., and Ahlf, J., "Comparison of Experimental 41J Shifts with the Predictions of German KTA 3203 and U.S. NRC Regulatory Guide 1.99," *Effects of Radiation on Materials: 14th International Symposium, ASTM STP 1046*, N.H. Packin, R.E. Stoller, and A.S. Kumar, Eds., American Society for Testing and Materials, Philadelphia, 1990, pp. 265-283.
Ishino 90	X			X	11	Ishino S, Kawakami T, Hidaka T, and Satoh M., "The effect of chemical composition on

Short Identifier	Embrittlement Shift Metric		Reactor Type		Number of Shift Data	Full Citation
	ΔT_{30}	ΔYS	Power	Test		
						irradiation embrittlement," *Nucl Eng Des* 1990(119): 139–48.
Pachur 93	X			X	5	Pachur, D., "Comparison of Drop-Weight and Instrumented Charpy Impact Test Results for Irradiated RPV," *Effects of Radiation on Materials: 16th International Symposium, ASTM STP 1175*, A.S. Kumar, D.S. Gelles, R.K. Nanstad, and E.A. Little, Eds., American Society for Testing and Materials, Philadelphia, 1993, pp. 195-210.
Leitz 93	X			X	5	Leitz, C., Klausnitzer, E.N., and Hofmann, G., "Annealing Experiments on Irradiated NiCrMo Weld Metal," *Effects of Radiation on Materials: 16th International Symposium, ASTM STP 1175*, A.S. Kumar, D.S. Gelles, R.K. Nanstad, and E.A. Little, Eds., American Society for Testing and Materials, Philadelphia, 1993, pp. 352-362.
Onizawa 01	X			X	8	Onizawa, K., and Suzuki, M., "Comparison of Transition Temperature Shifts Between Static Fracture Toughness and Charpy-v Impact Properties Due to Irradiation and Post-Irradiation Annealing for Japanese A533B-1 Steels," *Effects of Radiation on Materials: 20th International Symposium, ASTM STP 1405*, S.T. Rosinski, M.L. Grossbeck, T.R. Allen, and A.S. Kumar, Eds., American Society for Testing and Materials, West Conshohcken Pennsylvania, 2001, pp. 79-96.
Lee 01	X			X	2	Lee, B-S., Yang, W-J., Huh, M-Y., Chi, S-H., and Hong, J-H.,"Master Curve Characterization of Irradiation Embrittlement Using Standard and 1/3-Sized Precracked Charpy Specimens," *Effects of Radiation on Materials: 20th International Symposium, ASTM STP 1405*, S.T. Rosinski, M.L. Grossbeck, T.R. Allen, and A.S. Kumar, Eds., American Society for Testing and Materials, West Conshohcken Pennsylvania, 2001, pp. 55-67.
Nanstad 04	X			X	4	Nanstad, R.K., et al., "Fracture Toughness, Thermo-Electric Power, and Atom Probe Investigations of JRQ Steel in I, IA, IAR, and IARA Conditions," *Effects of Radiation on Materials: 22nd International Symposium, ASTM STP 1475*, T.R. Allen, R.G. Lott, J.T. Busby, and A.S. Kumar, Eds., American Society for Testing and Materials, West Conshohcken Pennsylvania, 2006, pp. 195-211.
Gérard 06		X	X	X	56	Gérard, R., E. Lucon, M.Scibetta, R.Chaouadi, and E. Van Walle, "Reactor Pressure Vessel Steels Embrittlement at Very High Neutron Doses," *Fontevraud 6th International Symposium on Contribution of Material Investigations to Improve Safety and Performance of LWRs*, September 18–22, 2006, Fontevraud-L'Abbaye, France.
RADAMO 05		X		X	358	R. Chaouadi, "An Engineering Radiation Hardening Model for RPV Materials," SCK/CEN Report R-4235, September 2005.
JNES 07	X			X	99	JNES-SS-0707, "Accuracy and Reliability of the Revised Transition Temperature Shift Prediction in the Japan Electrical Association Code, to be published.
Note: In many cases ΔYS data were also reported. These data were not considered as part of this analysis unless ΔT_{30} data were not available.						

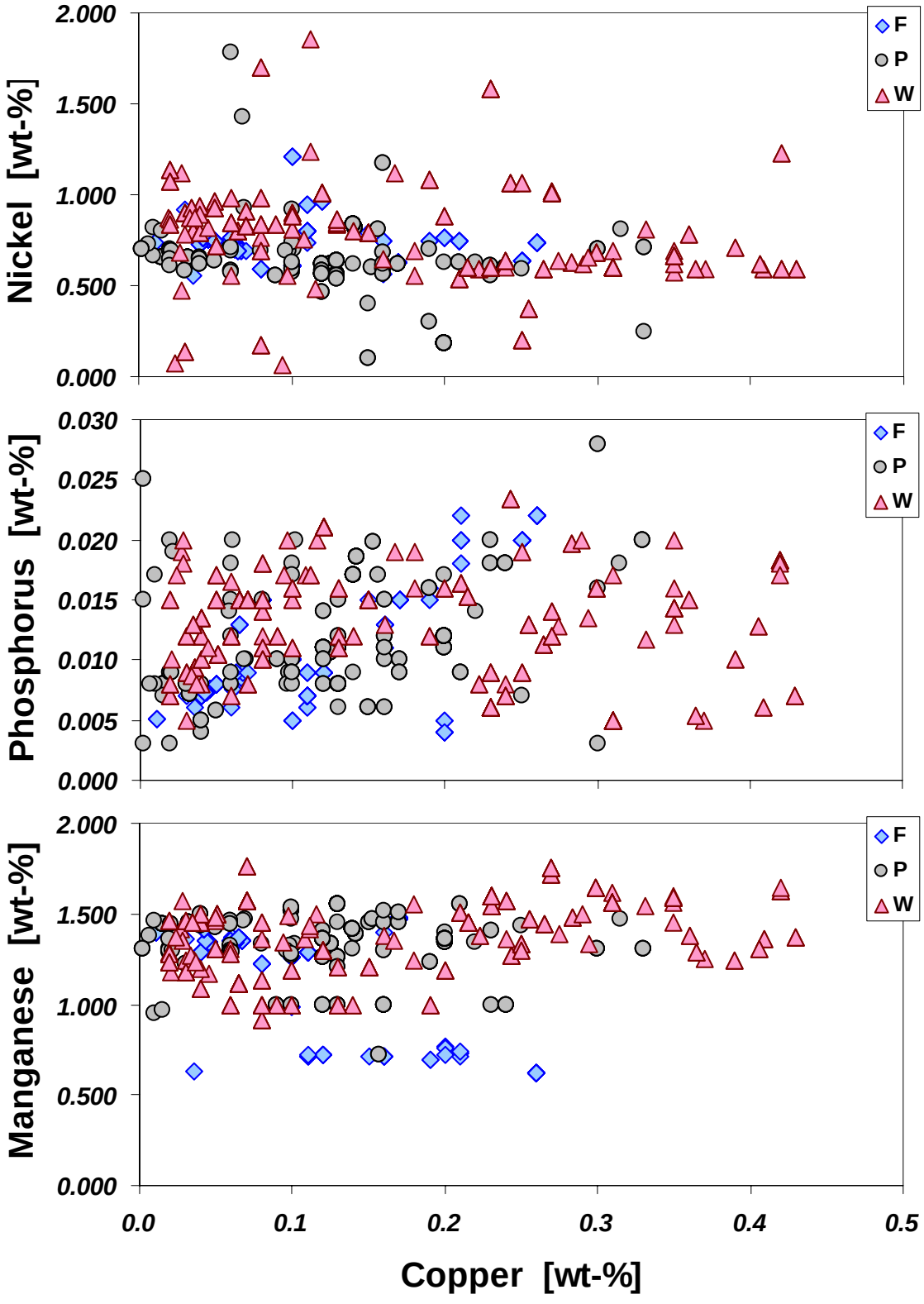

Figure G-2. Distribution of chemical composition in the high-fluence database taken from the literature.

Figure G-5 and Figure G-6 provide the same comparisons as were made on Figure G-4, but for forgings and welds, respectively. The trends discussed previously for the plate data are broadly consistent for all product forms, specifically:

- Model RM-6(2) provides a good representation of embrittlement trends at the low fluences that characterize the bulk of the US-LWR database. However, as fluence increases beyond $\approx 3 \times 10^{19}$ n/cm^2, RM-6(2) becomes less accurate, under-estimating the magnitude of embrittlement by progressively larger amounts as fluence increases.
- The ΔT_{30} model that was recommended in the main body of this report for use in Revision 3 of Regulatory Guide 1.99 incorporates a high fluence correction that was based on the RADAMO data. This model makes accurate predictions of embrittlement trends across the entire spectrum of fluences contained in the database assembled in this Appendix. This database reveals the recommended model to be accurate within the stated uncertainty bounds for fluences as high as $\approx 1.6 \times 10^{20}$ n/cm^2. However, as noted in the main body of this report, application of this model should be limited to steels having nickel contents below 1.25 wt-%.
- The database assembled here contains many more shift values obtained under the high flux conditions characteristic of test reactors than under the low flux conditions characteristic of power reactors. Nevertheless, comparison of the low flux to the high flux data reveals consistent trends between these two conditions. There is no effect of flux on embrittlement in these data that is significant enough to emerge from the background scatter that is characteristic of both the USLWR and the high-fluence databases.

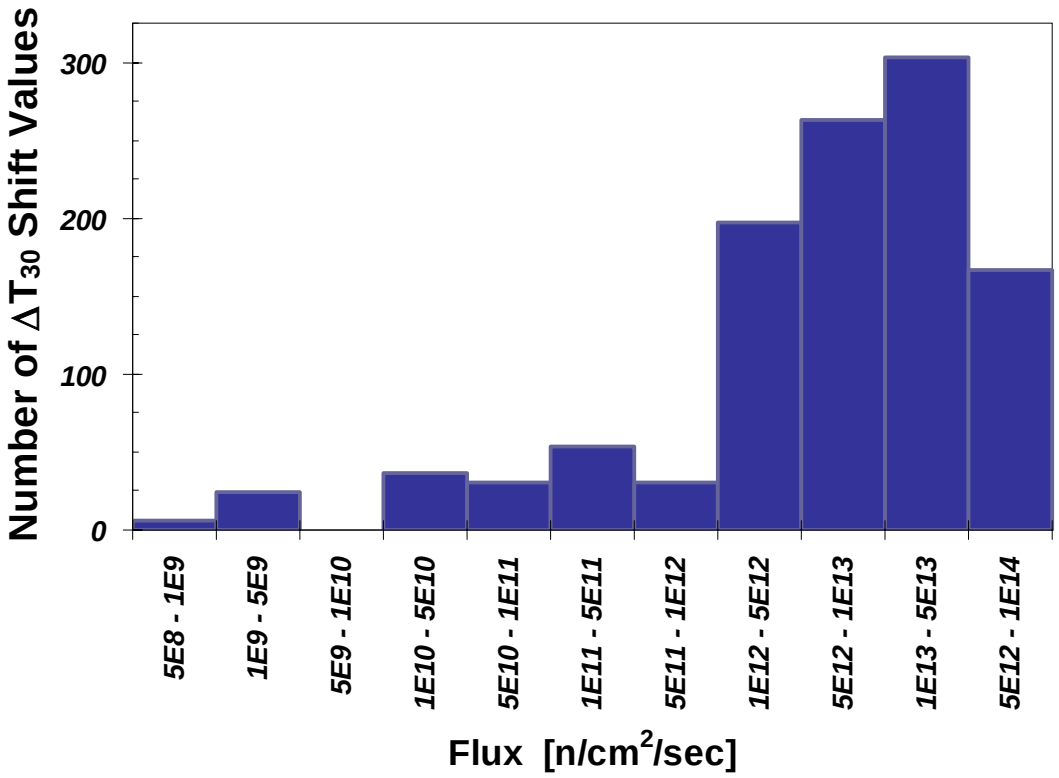

Figure G-3. Distribution of neutron flux in the high-fluence database taken from the literature.

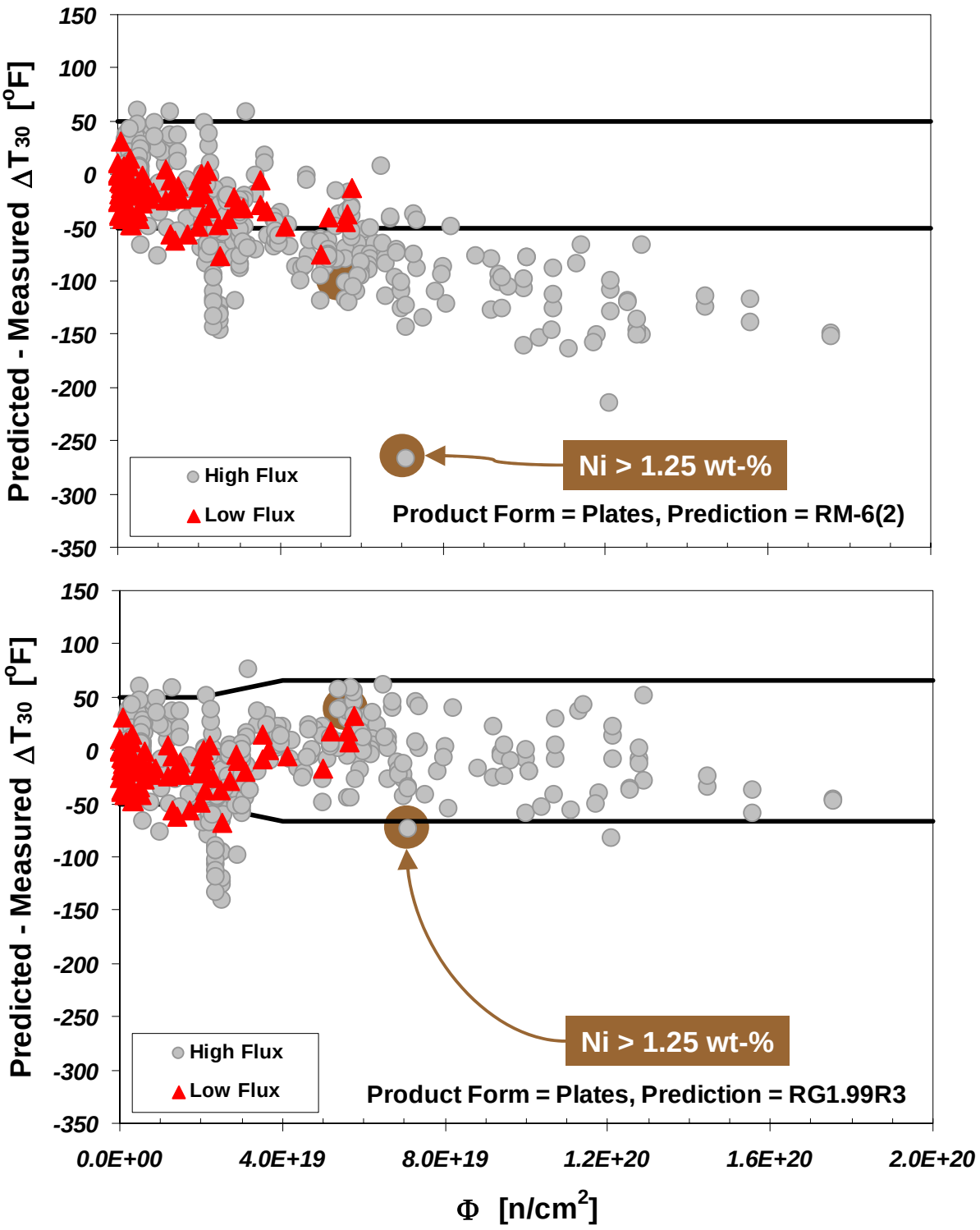

Figure G-4. Assessment of how well plates in the high-fluence database are predicted by (top) the ΔT_{30} model RM-6(2), which was calibrated only to US-LWR surveillance data, and by (bottom) the ΔT_{30} model recommended for use in Revision 3 of Regulatory Guide 1.99. The horizontal lines indicate $\pm 2\sigma$ confidence bounds, and the brown circles indicate two shift value having high nickel content.

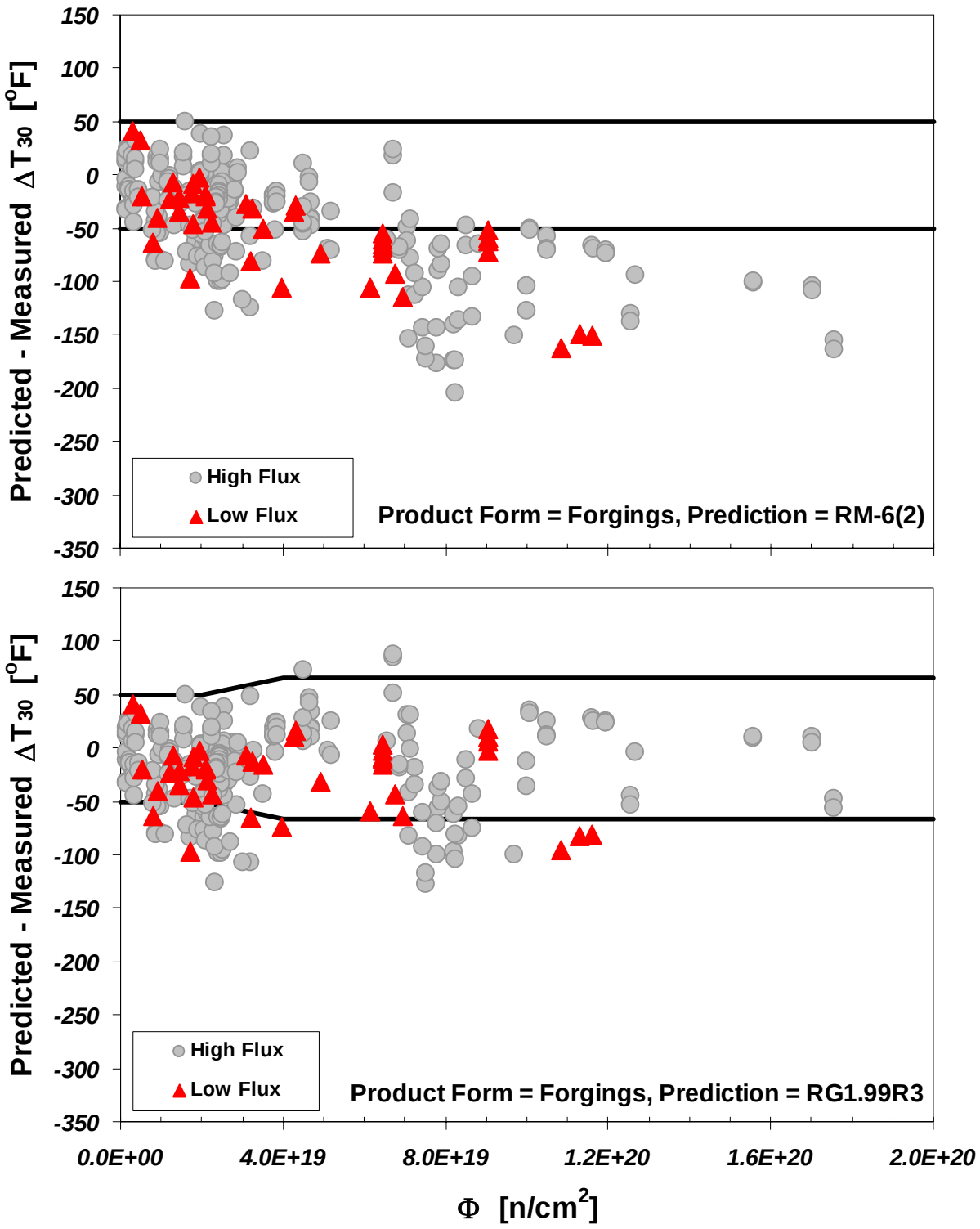

Figure G-5. Assessment of how well forgings in the high-fluence database are predicted by (top) the ΔT_{30} model RM-6(2), which was calibrated only to US-LWR surveillance data, and by (bottom) the ΔT_{30} model recommended for use in Revision 3 of Regulatory Guide 1.99. The horizontal lines indicate $\pm 2\sigma$ confidence bounds.

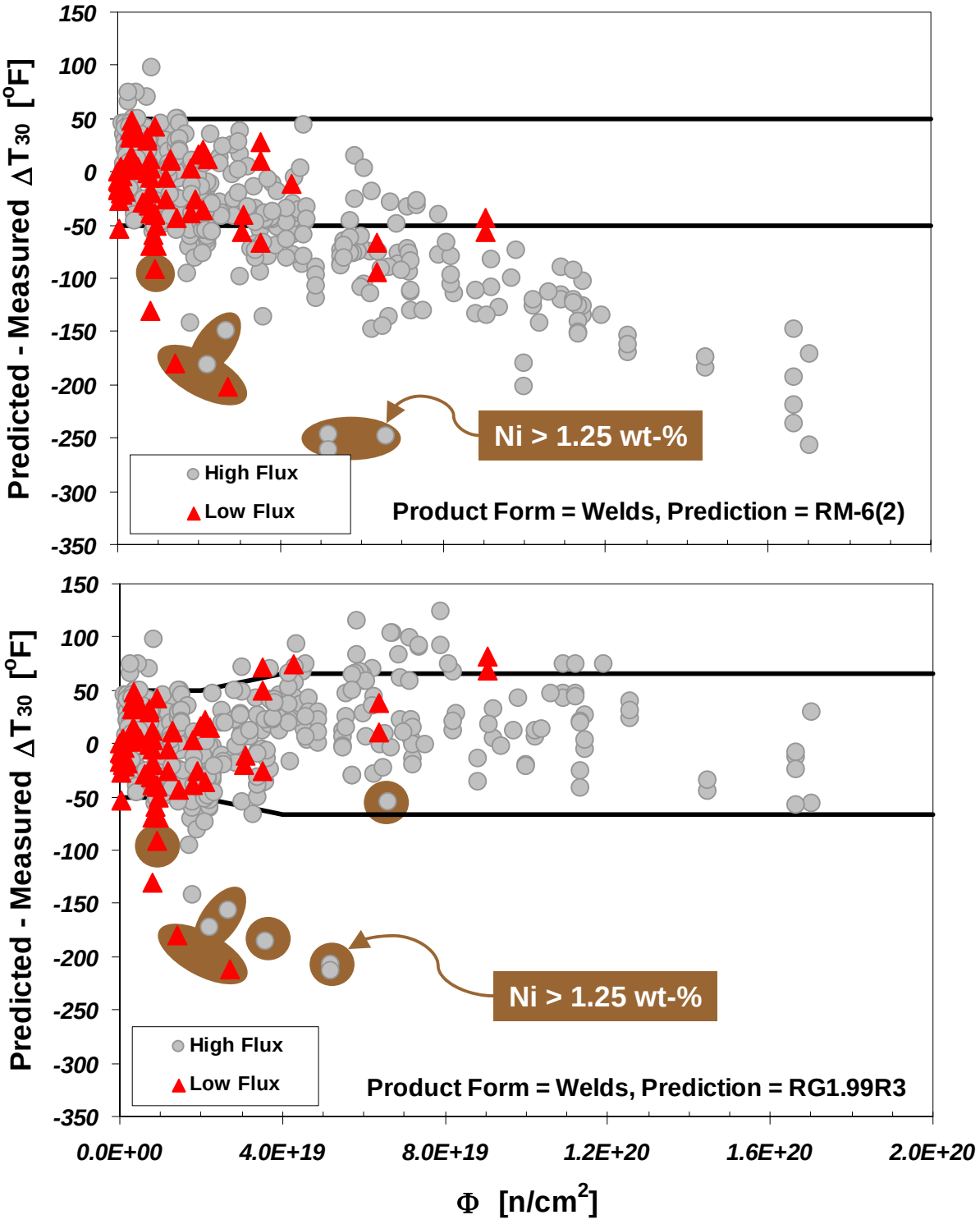

Figure G-6. Assessment of how well plates in the high-fluence database are predicted by (top) the ΔT_{30} model RM-6(2), which was calibrated only to US-LWR surveillance data, and by (bottom) the ΔT_{30} model recommended for use in Revision 3 of Regulatory Guide 1.99. The horizontal lines indicate $\pm 2\sigma$ confidence bounds, and the brown circles/ovals indicate shift values having high nickel content.

4 Summary and Recommendations

The comparisons presented in this Appendix demonstrate that the surveillance-calibrated ΔT_{30} ETC RM-6(2) represents available data well at low fluences (notionally less than $3x10^{19}$ n/cm^2). This finding is true irrespective of flux at which the data were collected. However, as fluence increases above $3x10^{19}$ n/cm^2 RM-6(2) begins to under-predict observed ΔT_{30} values, with the magnitude of under-prediction increasing as fluence increases. The bulk of the data summarized in this Appendix was collected in test reactors and, therefore, at fluxes above those experienced in power reactors at surveillance and vessel wall positions. Nevertheless, the limited power reactor / lower flux data available at high fluences (16% of the database assembled here) are also under-predicted by RM-6(2), just like the data from test reactors that were obtained at much higher fluxes. These findings support the following conclusions:

- RM-6(2), which was calibrated using only to the currently available surveillance data does not accurately represent data trends at high fluences (above $3x10^{19}$ n/cm^2). At higher fluences this model begins to under-predict observed ΔT_{30} values, with the magnitude of under-prediction increasing as fluence increases.
- The flux at which the ΔT_{30} data were obtained does not explain the under prediction observed in model RM-6(2).
    - At low fluences (notionally less than $3x10^{19}$ n/cm^2), all data are accurately predicted regardless of flux. These are mostly power reactor data (lower flux) but they include some test reactor data (higher flux).
    - At higher fluences (notionally above $3x10^{19}$ n/cm^2), there is a trend of increasing under-prediction with increasing fluence. This trend persists regardless of flux. Higher fluence data include mostly test reactor data (higher flux) along with a lesser amount power reactor data (lower flux).
- The agreement of available data, irrespective of flux, with RM-6(2) at low fluences coupled with the increasing disagreement of available data (again irrespective of flux) with RM-6(2) as fluence increases suggests that the deficiency of the RM-6(2) model cannot be primarily attributed to an inadequacy in the model's representation of flux effects. Since flux is not a determining factor in explaining model RM-6(2)'s tendency to under-predict embrittlement at high fluences, it seems justified to combine the more abundant test reactor data with the power reactor data at high fluences to inform a ΔT_{30} trend curve for use in the high fluence regime. In the main body of this report, a ΔT_{30} model was developed based on this approach, and this model was recommended for adoption in Revision 3 of Regulatory Guide 1.99. The recommended model adopts a high fluence correction that was based on the RADAMO data. The database assembled in this Appendix reveals the recommended model to be accurate within the stated uncertainty bounds in comparison with 1100+ shift values taken from the literature for fluences as high as $\approx 1.6x10^{20}$ n/cm^2. However, as noted in the main body of this report, application of the recommended model should be limited to steels having nickel contents below 1.25 wt-%.

In summary, the database of 1100+ ΔT_{30} and ΔYS shift values assembled in this Appendix provides additional information that supports adopting the ΔT_{30} model that was recommended in the main body of this report for Revision 3 of Regulatory Guide 1.99.

5 References

Bellmann 90 — Bellmann, D., and Ahlf, J., "Comparison of Experimental 41J Shifts with the Predictions of German KTA 3203 and U.S. NRC Regulatory Guide 1.99," *Effects of Radiation on Materials: 14th International Symposium, ASTM STP 1046,* N.H. Packin, R.E. Stoller, and A.S. Kumar, Eds., American Society for Testing and Materials, Philadelphia, 1990, pp. 265-283.

Brillaud 92 — Brillaud, C., and Hedin, F., "In-Service Evaluation of French Pressurized-Water Reactor Vessel Steel," *Effects of Radiation on Materials, 15th International Symposium,* ASTM STP-1125, R.E. Stoller, A.S. Kumar, and D.S. Gelles, Eds., American Society for Testing and Materials, 1992, pp. 23–49.

Brillaud 01 — Brillaud, C., Grandjean, Y., and Saillet, S., "Vessel Investigation Program of 'CHOOZ A' PWR Reactor after Shutdown," *Effects of Radiation on Materials: 20th International Symposium, ASTM STP 1405,* S.T. Rosinski, M.L. Grossbeck, T.R. Allen, and A.S. Kumar, Eds., American Society for Testing and Materials, West Conshohcken Pennsylvania, 2001, pp. 28-41.

Chaouadi 05 — R. Chaouadi, and R. Gérard, "Copper Precipitate Hardening of Irradiated RPV Materials and Implications on the Superposition Law and Re-Irradiation Kinetics," *Journal of Nuclear Materials,* **345** (2005), pp. 65–74.

Fabry 95 — Fabry, A., et al., "Research to Understand the Embrittlement Behavior of Yankee/BR3 Surveillance Plate and Other Outlier RPV Steels," *Effects of Radiation on Materials: 17th International Symposium, ASTM STP 1270,* D.S. Gelles, R.K. Nanstad, A.S. Kumar, and E.A. Little, Eds., American Society for Testing and Materials, Philadelphia, 1995, pp. 138-187.

Gérard 06 — Gérard, R., E. Lucon, M.Scibetta, R.Chaouadi, and E. Van Walle, "Reactor Pressure Vessel Steels Embrittlement at Very High Neutron Doses," *Fontevraud 6th International Symposium on Contribution of Material Investigations to Improve Safety and Performance of LWRs*, September 18–22, 2006, Fontevraud-L'Abbaye, France

Hawthorne 85 — Hawthorne, J.R., Menke, B.H., and Hiser, A.L., "Notch Ductility and Fracture Toughness Degradation of Pressure Vessel Steel Reference Plates from Pool Side Facility (PSF) Irradiation Capsules," *Effects of Radiation on Materials: 12th International Symposium, ASTM STP 870,* F.A. Garner and J.S. Perrin, Eds., American Society for Testing and Materials, Philadelphia, 1985, pp. 1163-1186.

IAEA 75 — IAEA-176, "Co-ordinated Research Programme on Irradiation Embrittlement of Pressure Vessel Steels," International Atomic Energy Agency, 1975.

IAEA 86 — TRS-265, "Analysis of the Behaviour of Advanced Reactor Pressure Vessel Steels under Neutron Irradiation," 1986.

IAEA CRP-3 — Unpublished Report and Database: Optimizing of Reactor Pressure Vessel Surveillance Programmes and their analyses

Ishino 90 — Ishino S, Kawakami T, Hidaka T, and Satoh M., "The effect of chemical composition on irradiation embrittlement," *Nucl Eng Des* 1990(119): 139–48.

JNES 07 JNES-SS-0707, “Accuracy and Reliability of the Revised Transition Temperature Shift Prediction in the Japan Electrical Association Code, to be published.

Kussmaul 90 Kussmaul, K., Föhl, J., and Weissenberg, T., “Investigation of Materials from a Decommissioned Reactor Pressure Vessel – A Contribution to the Understanding of Irradiation Embrittlement,” *Effects of Radiation on Materials: 14th International Symposium, ASTM STP 1046,* N.H. Packin, R.E. Stoller, and A.S. Kumar, Eds., American Society for Testing and Materials, Philadelphia, 1990, pp. 80-104.

Lee 01 Lee, B-S., Yang, W-J., Huh, M-Y., Chi, S-H., and Hong, J-H.,”Master Curve Characterization of Irradiation Embrittlement Using Standard and 1/3-Sized Precracked Charpy Specimens,” *Effects of Radiation on Materials: 20th International Symposium, ASTM STP 1405,* S.T. Rosinski, M.L. Grossbeck, T.R. Allen, and A.S. Kumar, Eds., American Society for Testing and Materials, West Conshohcken Pennsylvania, 2001, pp. 55-67.

Leitz 93 Leitz, C., Klausnitzer, E.N., and Hofmann, G., “Annealing Experiments on Irradiated NiCrMo Weld Metal,” *Effects of Radiation on Materials: 16th International Symposium, ASTM STP 1175,* A.S. Kumar, D.S. Gelles, R.K. Nanstad, and E.A. Little, Eds., American Society for Testing and Materials, Philadelphia, 1993, pp. 352-362.

Nanstad 04 Nanstad, R.K., et al., “Fracture Toughness, Thermo-Electric Power, and Atom Probe Investigations of JRQ Steel in I, IA, IAR, and IARA Conditions,” *Effects of Radiation on Materials: 22nd International Symposium, ASTM STP 1475,* T.R. Allen, R.G. Lott, J.T. Busby, and A.S. Kumar, Eds., American Society for Testing and Materials, West Conshohcken Pennsylvania, 2006, pp. 195-211.

Onizawa 01 Onizawa, K., and Suzuki, M., “Comparison of Transition Temperature Shifts Between Static Fracture Toughness and Charpy-V Impact Properties Due to Irradiation and Post-Irradiation Annealing for Japanese A533B-1 Steels,” *Effects of Radiation on Materials: 20th International Symposium, ASTM STP 1405,* S.T. Rosinski, M.L. Grossbeck, T.R. Allen, and A.S. Kumar, Eds., American Society for Testing and Materials, West Conshohcken Pennsylvania, 2001, pp. 79-96.

Pauchur 93 Pauchur, D., “Comparison of Drop-Weight and Instrumented Charpy Impact Test Results for Irradiated RPV,” *Effects of Radiation on Materials: 16th International Symposium, ASTM STP 1175,* A.S. Kumar, D.S. Gelles, R.K. Nanstad, and E.A. Little, Eds., American Society for Testing and Materials, Philadelphia, 1993, pp. 195-210.

Stallmann 94 E W. Stallmann, J. A. Wang, E B. K. Kam, “TR-EDB: Test Reactor Embrittlement Data Base, Version 1,” NUREG/CR-6076, United States Nuclear Regulatory Commission, 1994

ANNEX 1

In this Annex to Appendix G the data obtained from each literature citation are compared to the trend curves developed in the main body of this document; the comparison for each data set is structured as follows:

- First the data from the citation is identified as falling into one of the following three categories:
  - Only high flux / test reactor data
  - Only low flux / power reactor data
  - Both high and low flux data (i.e., both test and power reactor irradiations)
- Second the source of the data, material, test, and irradiation conditions are described briefly, making use of a consistent tabular format. In situations where assumptions had to be made to enable comparison of the published data with the predictions of the trend curve this is called out and explained.
- Third the data are compared with trend curve RM-6(2), which was developed by fitting only the ΔT_{30} data in the US LWR surveillance database. In situations where only ΔYS data are available for comparison, the ΔYS values (which have units of MPa) are converted to ΔT_{30} values (which have units of °F) using the following formula, which appeared as Eq. 4-19 in the main text:

$$\Delta T_{30} = \left\{ \begin{array}{c} Weld = 1.39 \\ Plate = 1.18 \\ Forging = 0.84 \end{array} \right\} \cdot \Delta YS$$

  Based on the information presented in the main text the expectation is that the measured ΔT_{30} values will compare favorably with the predictions of RM-6(2) at fluences below $\approx 3 \times 10^{19}$ n/cm^2, but that RM-6(2) will begin to under-predict measured ΔT_{30} values as fluence increases above this value.
- Finally the data are compared with trend curve that was recommended in the main text for adoption in Revision 3 or Regulatory Guide 1.99, which consists of RM-6(2) at low fluences and an ETC that was based on the RADAMO data at higher fluences (this equation is described in Section 4.5 of the main text). If only ΔYS data are available for comparison, the ΔYS values are converted to ΔT_{30} values using the procedure just described. Based on the information presented in the main text the expectation is that the measured ΔT_{30} values will compare favorably with the predictions of this equation at all fluences.

Citation: **CRP-1**, IAEA-176, "Co-ordinated Research Programme on Irradiation Embrittlement of Pressure Vessel Steels," International Atomic Energy Agency, 1975.

In this investigation researchers from seven different countries irradiated the ASTM A533B reference material Plate 03 from the Oak Ridge National Laboratory (ORNL) Heavy Section Steel Technology (HSST). Exposures were made in a number of different test reactors and irradiation locations.

Table G.2. Summary materials and irradiation condition studied in CRP-1.

Short ID: CRP-1 Category: High Flux Only

Material	Product	Specification	Cu [wt-%]	Ni [wt-%]	P [wt-%]	Mn [wt-%]
HSST-03	Plate	ASTM A533B	0.13	0.56	0.011	1.26

Country	Reactor	Capsule Location	Irradiation Temperature [^{o}F]	Flux [n/cm^{2}/sec]	Notes
Japan	JMTR	1st later of reflector	531	6E+12	
	JRR-2	Vertical thimble 1	536	1E+13	
United Kingdom	DIDO (Heavy H_2O)	Mark 5/4 fuel element shield plug	554	1E+14	
France	TRITON	At core perimeter	554	5E+12	
Sweden	R2	Hot water loop	554	5E+13	Target flux
Denmark	DR-3 (Heavy H_2O)	In fuel element, center hole	554	5E+13	
Czechoslovakia	VVR-S	At core perimeter	545	1E+13	Estimated flux
Germany	FRJ-2 (DIDO Type, Heavy H_2O)	In fuel element	554	2E+13	

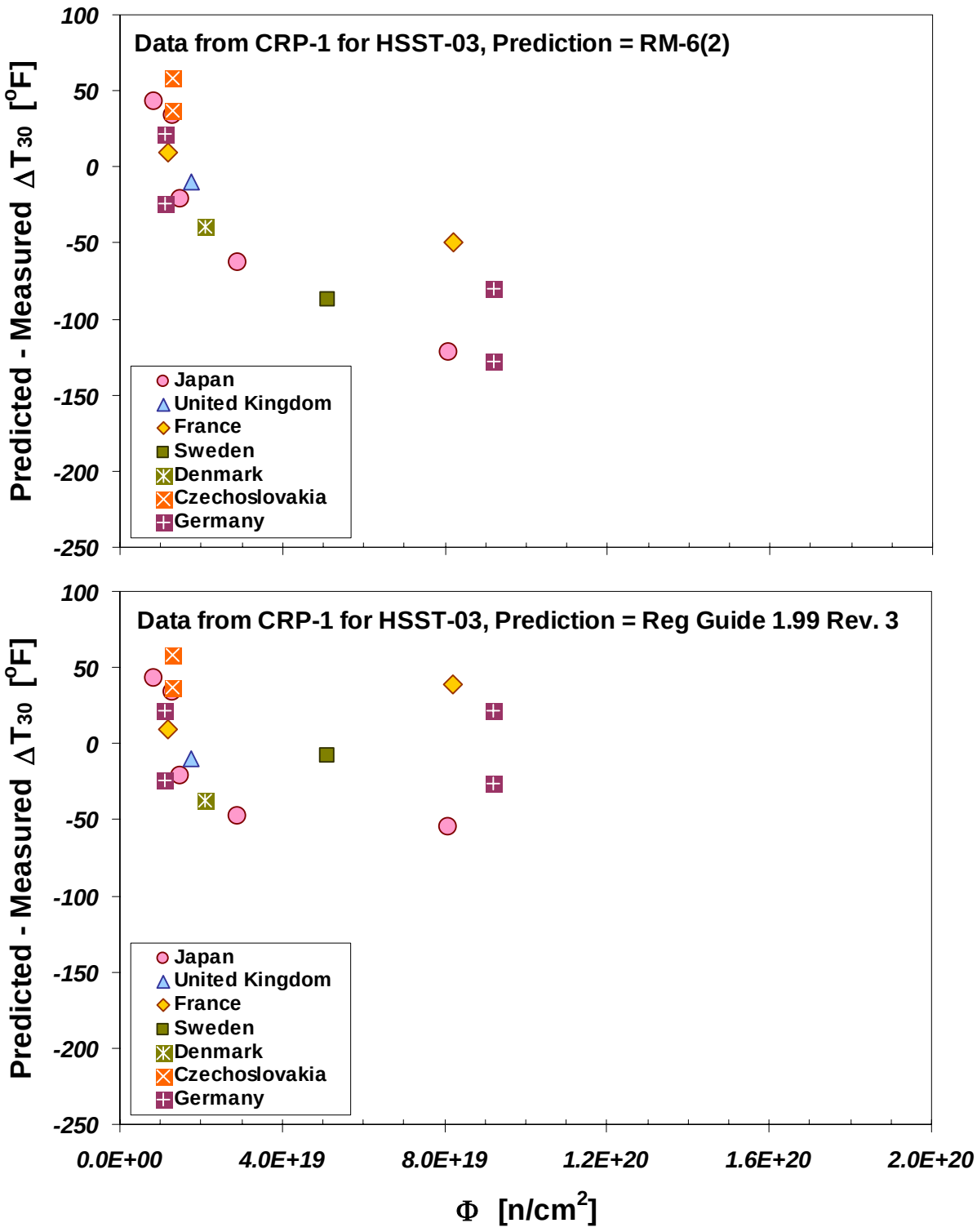

Figure G-7. Assessment of how well CRP-1 data are predicted by (top) the ΔT_{30} model RM-6(2), which was calibrated only to US-LWR surveillance data, and by (bottom) the ΔT_{30} model recommended for use in Revision 3 of Regulatory Guide 1.99.

Citation: **CRP-2**, TRS-265, "Analysis of the Behaviour of Advanced Reactor Pressure Vessel Steels under Neutron Irradiation," 1986.

In this investigation researchers from seven different countries irradiated eight different RPV steels and weldments in a number of different test reactors and irradiation locations. Data were reported for several irradiation temperatures, however in the comparisons presented here attention is focussed on irradiation exposures conducted at temperatures near 550 °F.

Table G.3. Summary materials and irradiation condition studied in CRP-2.

Short ID: CRP-2 Category: High Flux Only

Material	Product	Specification	Cu [wt-%]	Ni [wt-%]	P [wt-%]	Mn [wt-%]
FF	Forging	ASTM A508 Cl. 3	0.067	0.70	0.009	1.35
FP	Plate	ASTM A533B Cl. 1	0.032	0.65	0.007	1.46
FW	Weld	Sub Arc Weld	0.051	0.72	0.010	1.50
GW	Weld	Sub Arc Weld	0.040	0.93	0.014	1.46
HSST-03	Plate	ASTM A533B Cl. 1	0.125	0.62	0.011	1.33
JF	Forging	ASTM A508 Cl. 3	0.045	0.75	0.008	1.34
JP	Plate	ASTM A533B Cl. 1	0.015	0.65	0.008	1.44
JW	Weld	Sub Arc Weld	0.036	0.80	0.009	1.24

Country	Reactor	Capsule Location	Irradiation Temperature [°F]	Flux [n/cm^2/sec]	Materials Tested
Japan	JMTR (Light water)	Be-reflector	554	2E+13	FF, FP, FW, JF, JP, JW
United Kingdom	HERALD (Light water)	Be-reflector	554	3-5E+12	FF, JF, JW
France	TRITON & MELSUINE (both light water)	At core perimeter	547	1E+13	FF, FP, FW, GW, JF, JP, JW
India	CIRUS	Mid section of core	554	4E+12	FF, FP, FW, JF, JP
United States	UBR (Light water)	Core	550	Not Stated	FF, FP, FW, GW, HSST-03, JF,
Czechoslovakia	VVR-S (Light water)	At core perimeter	545	2E+13	FF, FP, FW, GW, JF, JP, JW
Germany	FRG-2 (Light water)	Reflector	554	4E+12 to 2.5E+13	FF, FP, GW, HSST-03, JF, JP
	VAK (Light water)	Near core		3E+12	
	KKS (Light water)	Surveillance		8E+11	
	FRJ-1 MERLIN (Light water)	Reflector		2E+12	
	FRJ-2 DIDO (Heavy water)	In fuel element		3E+13	

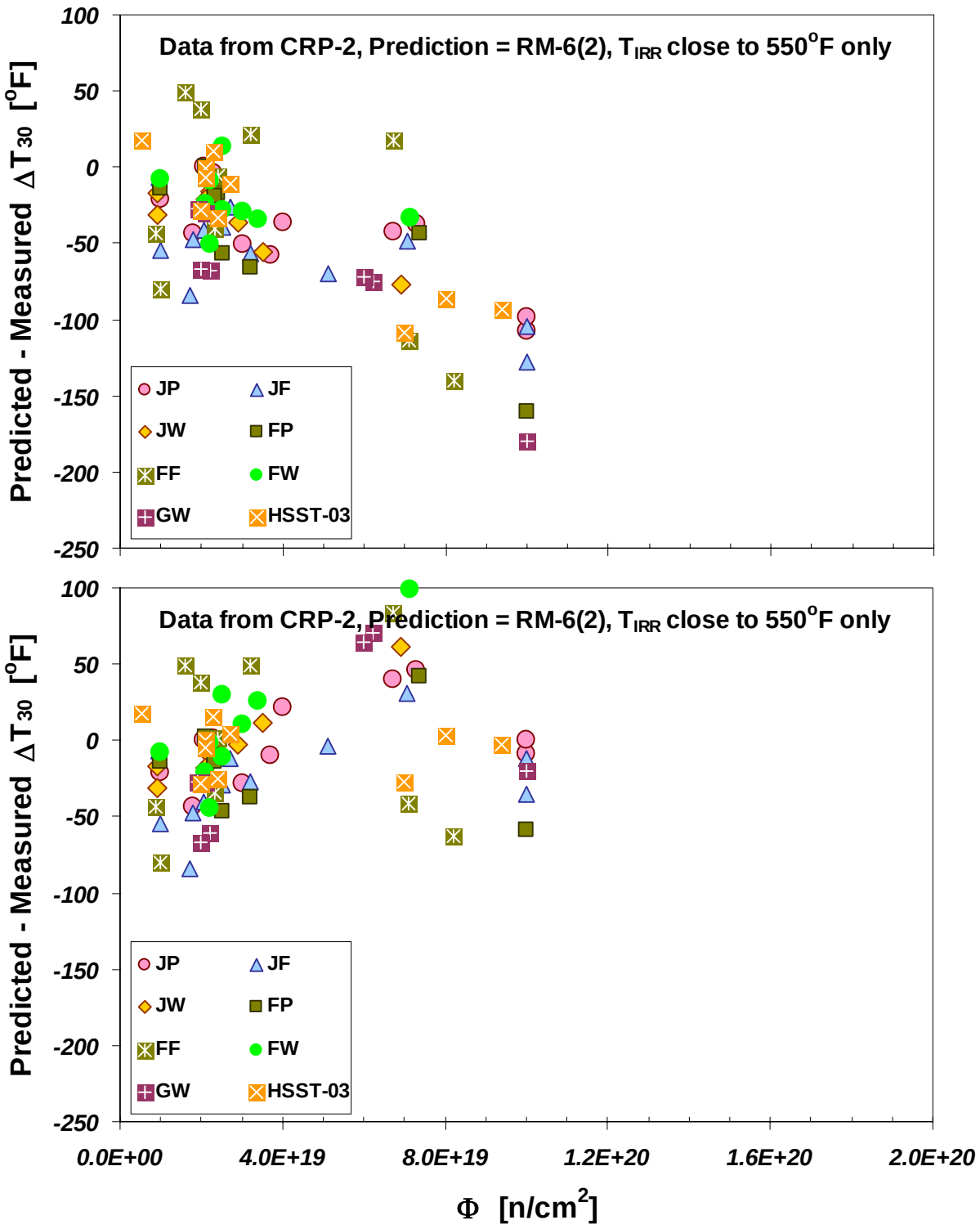

Figure G-8. Assessment of how well CRP-2 data are predicted by (top) the ΔT_{30} model RM-6(2), which was calibrated only to US-LWR surveillance data, and by (bottom) the ΔT_{30} model recommended for use in Revision 3 of Regulatory Guide 1.99.

Citation: **CRP-3**, Unpublished Report and Database: Optimizing of Reactor Pressure Vessel Surveillance Programmes and their Analyses

In this investigation researchers from several different countries irradiated a wide variety of RPV steels and weldments. Data were reported for several irradiation temperatures, however in the comparisons presented here attention is focussed on irradiation exposures conducted at temperatures near 550 °F. Information on flux, reactor type, and irradiation location were not given in the database. In previous CRPs fluxes ranging from of $\approx 10^{12}$ to $\approx 10^{14}$ n/cm^2/s were reported associated with test reactor irradiations. Figure G-9 demonstrates data trends are not altered by selection of assumed fluxes that throughout this range. A flux of 10^{13} n/cm^2/s was therefore used in Figure G-10 in the assessment of both the RM-6(2) model and the model recommended for use in Revision 3 of Regulatory Guide 1.99.

The data presented here were provided to the NRC by Dr. Ferenc Gillemot of the Hungarian Academy of Sciences' Atomic Energy Research Institute (AEKI). Dr. Gillemot maintains databases of the information obtained in the various CRP projects for the IAEA.

Table G.4. Summary materials and irradiation condition studied in CRP-3.

Short ID: CRP-3 Category: High Flux Only

Material	Product	Specification	Cu [wt-%]	Ni [wt-%]	P [wt-%]	Mn [wt-%]
FFA	Forging	ASTM A508 Cl. 3	0.060	0.71	0.006	1.30
JFL	Forging	ASTM A508 Cl. 3	0.011	0.73	0.005	1.40
JPA	Plate	ASTM A533B Cl. 1	0.315	0.81	0.018	1.47
JPB	Plate	ASTM A533B Cl. 1	0.010	0.82	0.017	0.95
JPC	Plate	ASTM A533B Cl. 1	0.015	0.80	0.007	0.97
JPD	Plate	ASTM A533B Cl. 1	0.150	0.10	0.006	1.45
JPE	Plate	ASTM A533B Cl. 1	0.150	0.40	0.006	Not stated
JPF	Plate	ASTM A533B Cl. 1	0.153	0.60	0.020	1.47
JPG	Plate	ASTM A533B Cl. 1	0.157	0.81	0.017	0.73
JPH	Plate	ASTM A533B Cl. 1	0.160	1.18	0.006	1.45
JPI	Plate	ASTM A533B Cl. 1	0.010	0.66	0.008	1.46
JPJ	Plate	ASTM A533B Cl. 1	0.050	0.63	0.006	1.42
JRQ	Plate	ASTM A533B Cl. 1	0.142	0.82	0.019	1.39
JWN	Weld	Sub Arc Weld	0.019	0.87	0.007	1.29
JWO	Weld	Sub Arc Weld	0.030	0.78	0.005	1.24
JWP	Weld	Sub Arc Weld	0.030	0.90	0.009	1.18
JWQ	Weld	Sub Arc Weld	0.243	1.06	0.023	1.27

Reactor	Capsule Location	Irradiation Temperature [^{o}F]	Flux [n/cm^2/sec]	Notes
See discussion in text				

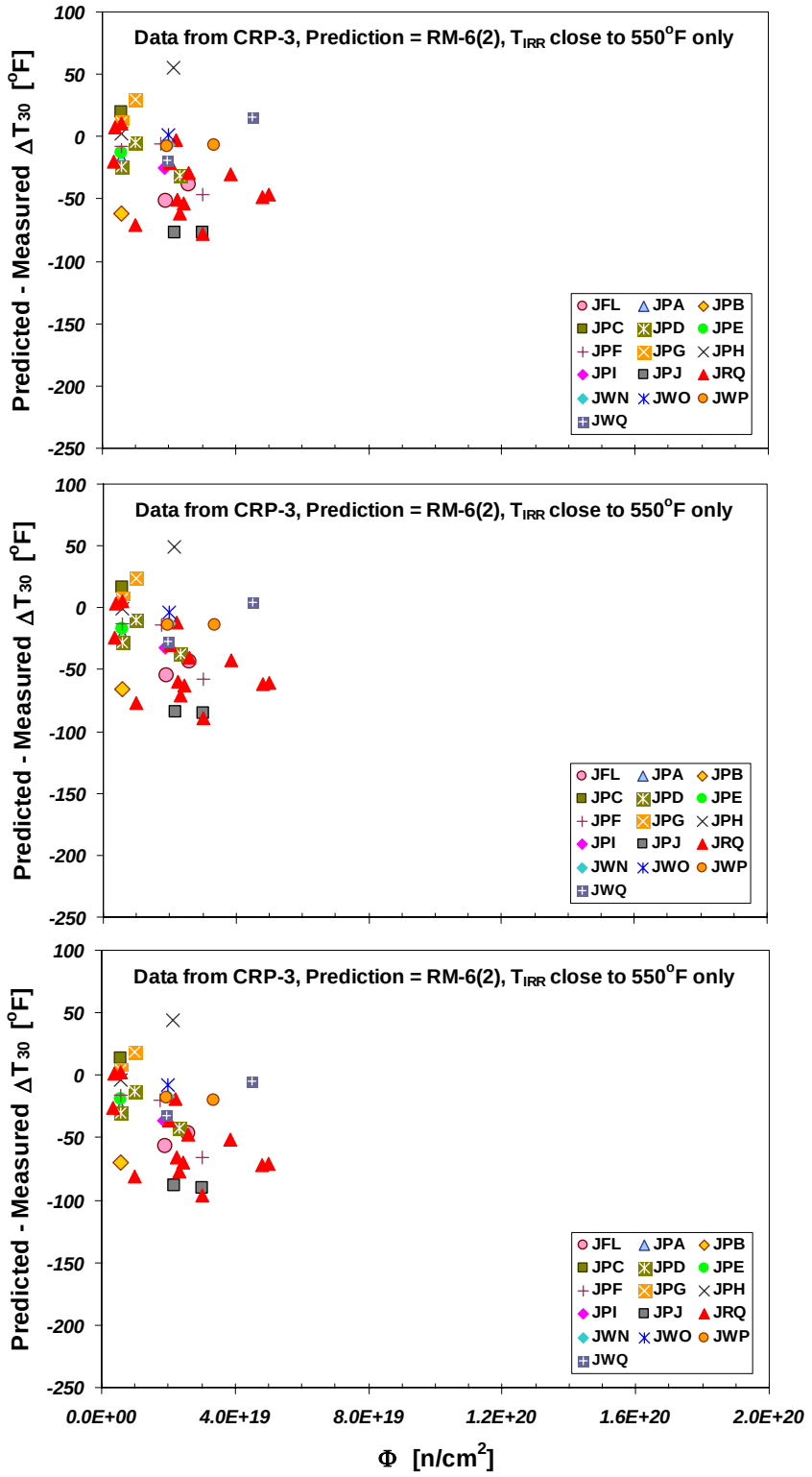

Figure G-9. Assessment of the effect of assumed flux on now well CRP-3 data are predicted by the ΔT_{30} model RM-6(2). In the top, middle, and bottom graphs the assumed flux was set equal to $1x10^{12}$, $1x10^{13}$, and $1x10^{14}$ n/cm^2/s, respectively.

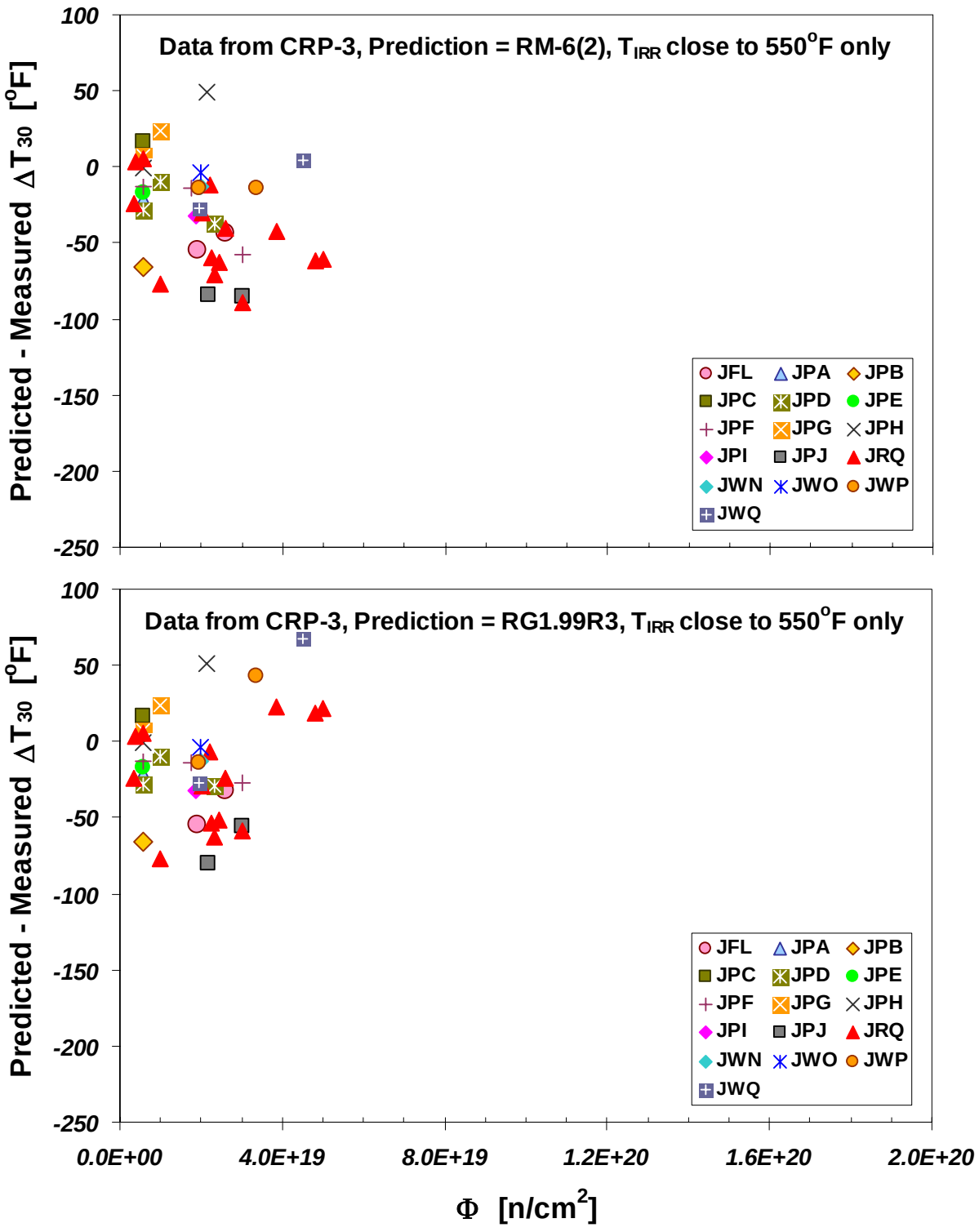

Figure G-10. Assessment of how well CRP-3 data are predicted by (top) the ΔT_{30} model RM-6(2), which was calibrated only to US-LWR surveillance data, and by (bottom) the ΔT_{30} model recommended for use in Revision 3 of Regulatory Guide 1.99. Assumed flux was 1×10^{13} n/cm^2/s.

Citation: **TR-EDB**, E W. Stallmann, J. A. Wang, E B., and K. Kam, "TR-EDB: Test Reactor Embrittlement Data Base, Version 1," NUREG/CR-6076, United States Nuclear Regulatory Commission, 1994.

In the early 1990s the NRC commissioned the HSST program at ORNL to compile a database of irradiation embrittlement data reported in studies other than power reactor surveillance studies. These data were compiled into a D-BASE database called "TR-EDB" (Test Reactor Embrittlement Data Base). After elimination of records having undefined flux and/or chemistry values, and after restricting attention to the calibrated temperature range of RM-6(2) a total of 269 ΔT_{30} records remained. Figure G-11shows the distribution of flux values for these data, while Figure G-12 illustrates their range of chemistry values.

Comparisons of the TR-EDB data to the predictions of the RM-6(2) model and the model recommended for use in Revision 3 of Regulatory Guide 1.99 are made in the following four figures:

- Figure G-13 for all chemistries and for all temperatures above 525 °F, with the plotting symbol indicating flux.
- Figure G-14 is the same as Figure G-13 except that the maximum nickel for the plot has been restricted to 1.25 wt-% because, as documented in the main text, RM-6(2) is known to under-predict the embrittlement magnitude in high nickel materials. Comparison of Figure G-14 to Figure G-13 demonstrates that it is the high nickel materials in TR-EDB that are the most under-predicted.
- Figure G-15 for all chemistries and for all temperatures above 525 °F, with the plotting symbol indicating product form.
- Figure G-16 is the same as Figure G-15 except that the maximum nickel for the plot has been restricted to 1.25 wt-% because, as documented in the main text, RM-6(2) is known to under-predict the embrittlement magnitude in high nickel materials. Comparison of Figure G-16 to Figure G-15 demonstrates that it is the high nickel materials in TR-EDB that are the most under-predicted.

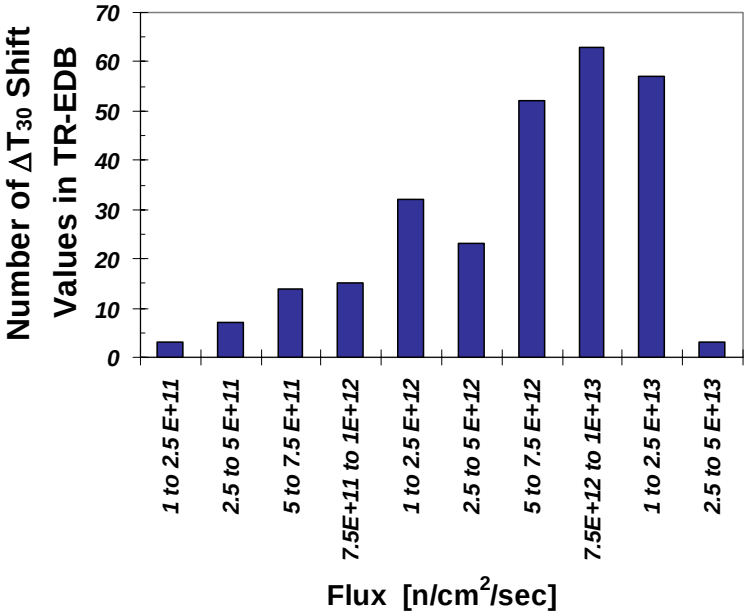

Figure G-11. Range of neutron flux values in TR-EDB.

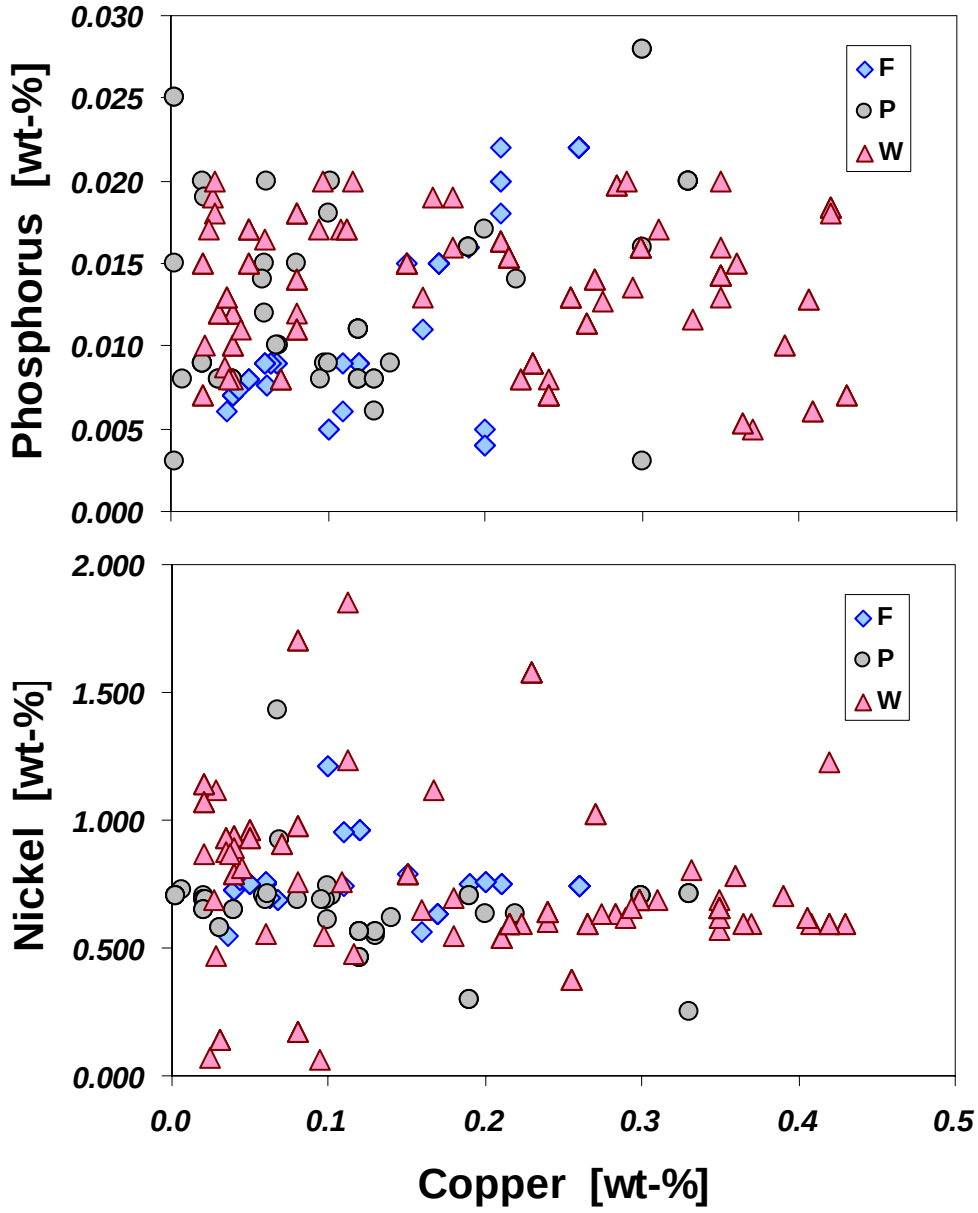

Figure G-12. Range of copper, nickel, and phosphorus contents in TR-EDB.

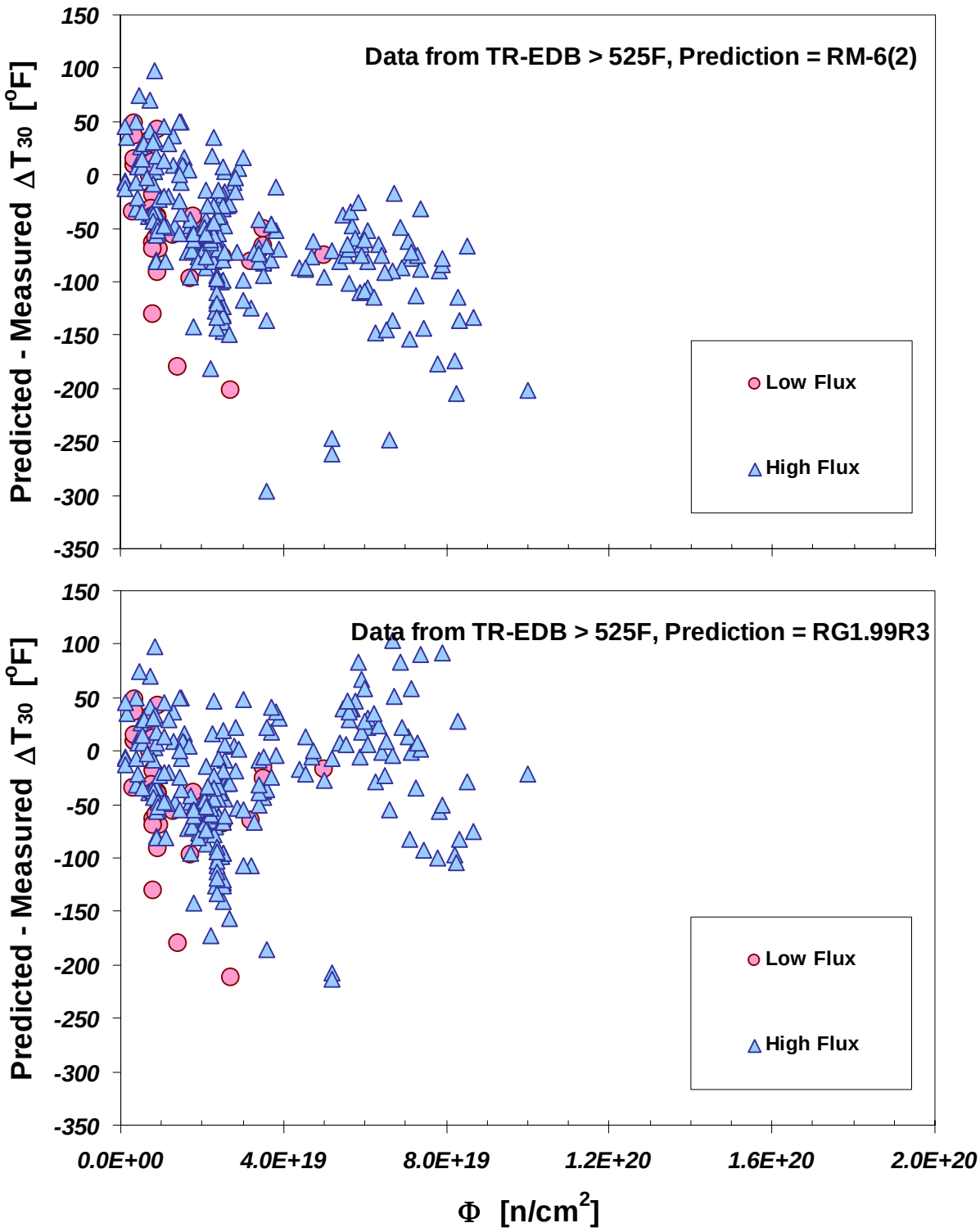

Figure G-13. Assessment of how well data from the TR-EDB database are predicted by (top) the ΔT_{30} model RM-6(2), which was calibrated only to US-LWR surveillance data, and by (bottom) the ΔT_{30} model recommended for use in Revision 3 of Regulatory Guide 1.99. Plots show the full nickel range in TR-EDB; division between low and high flux is made at 10^{12} n/cm^2/s.

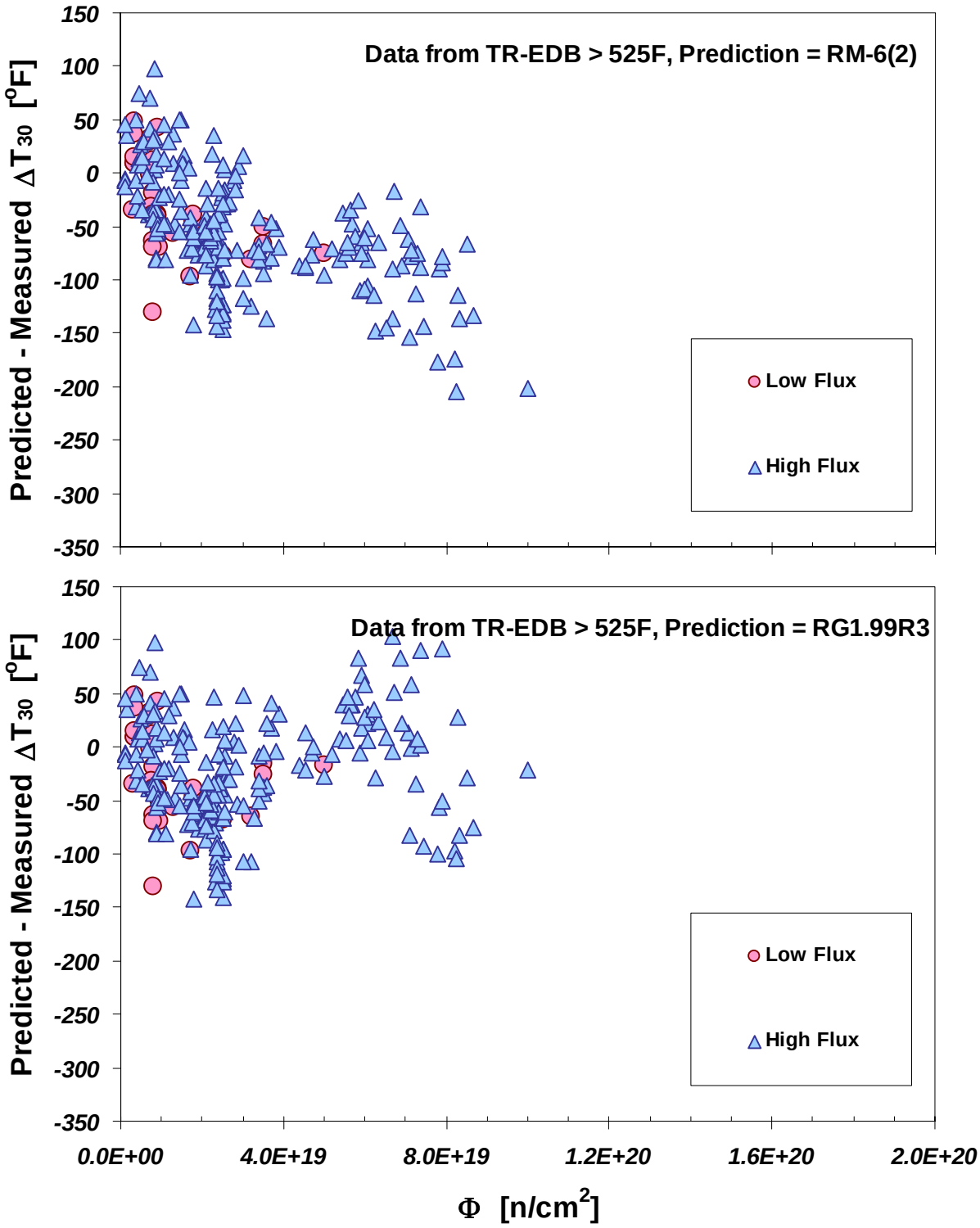

Figure G-14. Assessment of how well data from the TR-EDB database are predicted by (top) the ΔT_{30} model RM-6(2), which was calibrated only to US-LWR surveillance data, and by (bottom) the ΔT_{30} model recommended for use in Revision 3 of Regulatory Guide 1.99. In this figure nickel is limited to 1.25 wt-%; division between low and high flux is made at 10^{12} n/cm^2/s.

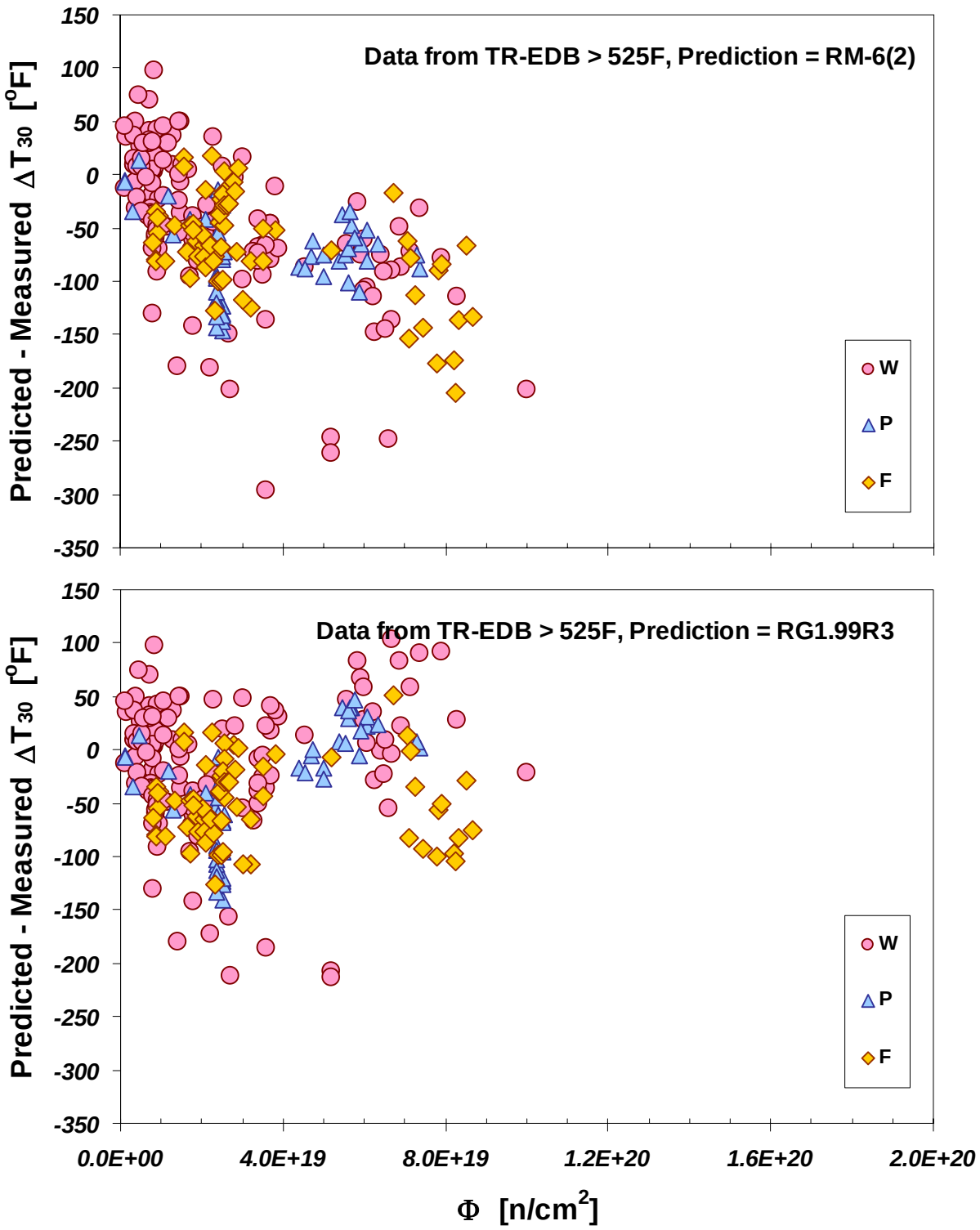

Figure G-15. Assessment of how well data from the TR-EDB database are predicted by (top) the ΔT_{30} model RM-6(2), which was calibrated only to US-LWR surveillance data, and by (bottom) the ΔT_{30} model recommended for use in Revision 3 of Regulatory Guide 1.99. Plots show the full nickel range in TR-EDB; division between low and high flux is made at 10^{12} n/cm^2/s.

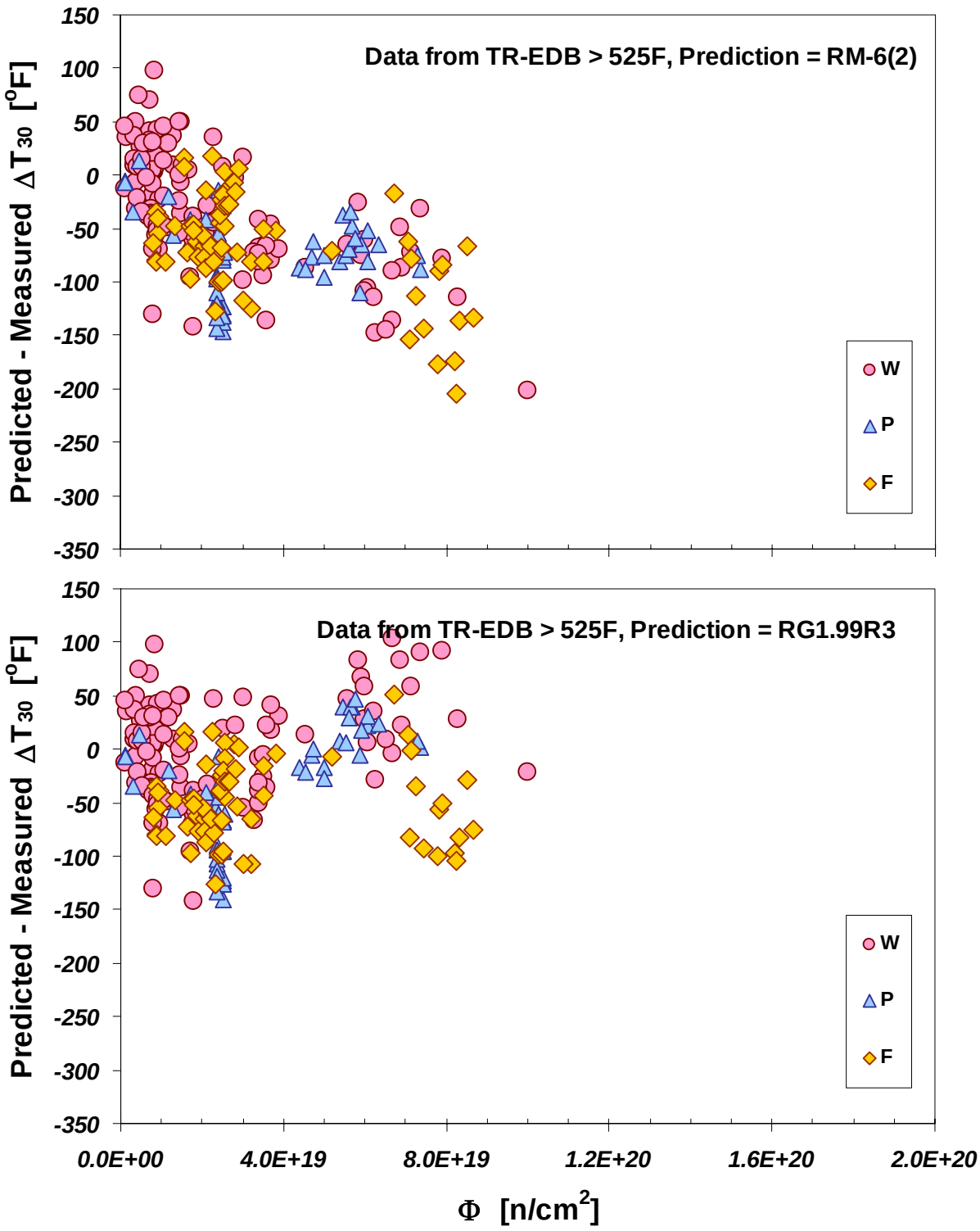

Figure G-16. Assessment of how well data from the TR-EDB database are predicted by (top) the ΔT_{30} model RM-6(2), which was calibrated only to US-LWR surveillance data, and by (bottom) the ΔT_{30} model recommended for use in Revision 3 of Regulatory Guide 1.99. In this figure nickel is limited to 1.25 wt-%; division between low and high flux is made at 10^{12} n/cm^2/s.

Citation: **Hawthorne 85**, Hawthorne, J.R., Menke, B.H., and Hiser, A.L., "Notch Ductility and Fracture Toughness Degradation of Pressure Vessel Steel Reference Plates from Pool Side Facility (PSF) Irradiation Capsules," *Effects of Radiation on Materials: 12th International Symposium, ASTM STP 870*, F.A. Garner and J.S. Perrin, Eds., American Society for Testing and Materials, Philadelphia, 1985, pp. 1163-1186.

In this investigation Hawthorne assesses the effect of flux level on two correlation monitor materials.

Table G.5. Summary materials and irradiation condition studied in Hawthorne 85.

Short ID: Hawthorne 85 Category: Low and High Flux

Material	Product	Specification	Cu [wt-%]	Ni [wt-%]	P [wt-%]	Mn [wt-%]
ASTM reference correlation monitor plate	Plate	ASTM A302B	0.2	0.18	0.011	1.34
HSST-03	Plate	ASTM A533B	0.12	0.56	0.011	1.26

Reactor	Capsule ID	Capsule Location	Irradiation Temperature [°F]	Flux [n/cm^2/sec]	Notes
PSF	SSC-1	Thernal shield	550.4	6.5E+12	Fluence same as Wall-2
	SSC-2	Thernal shield	550.4	5.9E+12	Fluence same as Wall-1
	Wall-1	Simulation of ID location	550.4	8.9E+11	Fluence same as SSC-2
	Wall-2	Simulation of 1/4-T location	550.4	4.4E+11	Fluence same as SSC-1
	Wall-3	Simulation of 1/2-T location	550.4	2.2E+11	

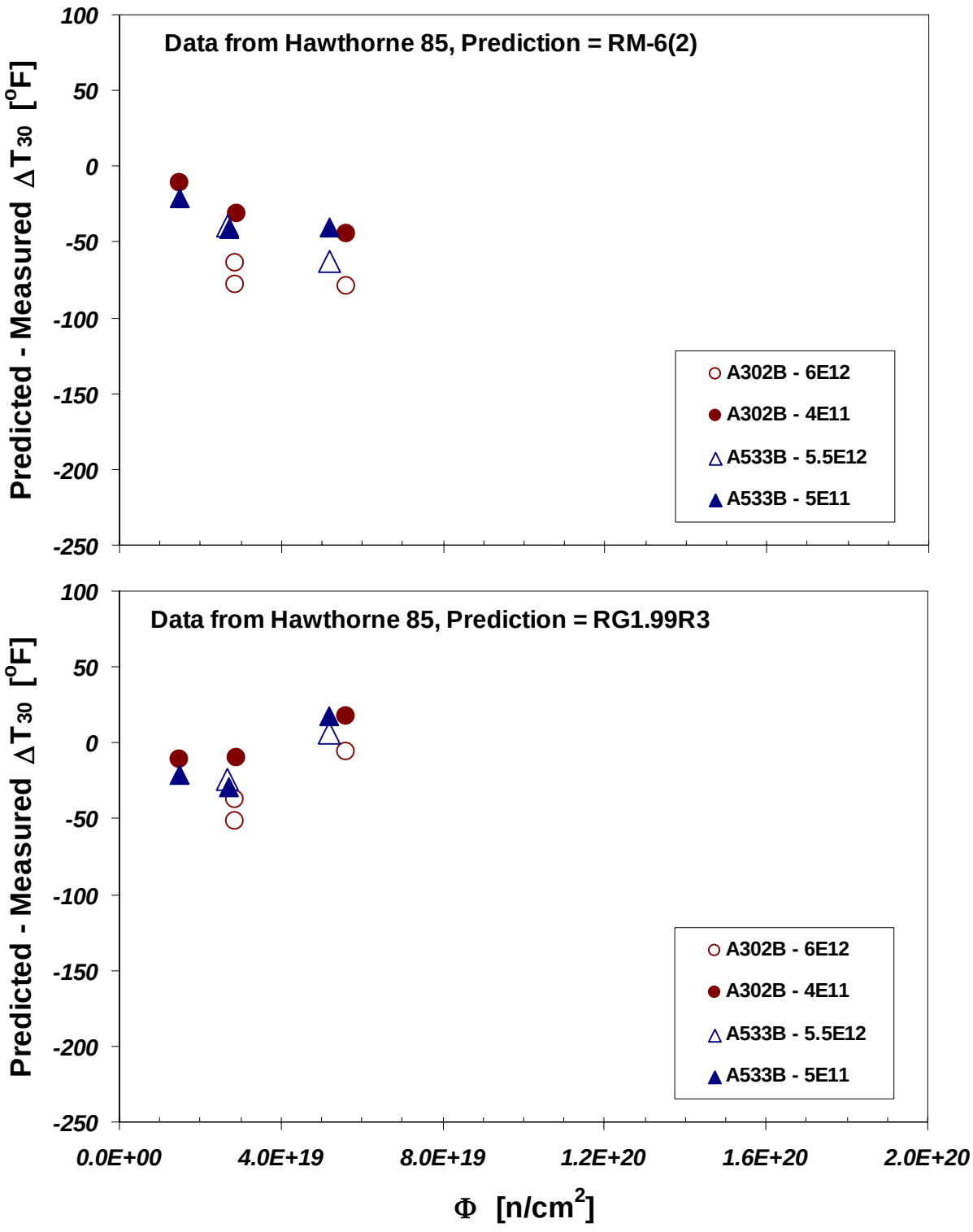

Figure G-17. Assessment of how well Hawthorne 85 data are predicted by (top) the ΔT_{30} model RM-6(2), which was calibrated only to US-LWR surveillance data, and by (bottom) the ΔT_{30} model recommended for use in Revision 3 of Regulatory Guide 1.99.

Citation: **Fabry 96**, Fabry, A., et al., "Research to Understand the Embrittlement Behavior of Yankee/BR3 Surveillance Plate and Other Outlier RPV Steels," *Effects of Radiation on Materials: 17th International Symposium, ASTM STP 1270*, D.S. Gelles, R.K. Nanstad, A.S. Kumar, and E.A. Little, Eds., American Society for Testing and Materials, Philadelphia, 1996, pp. 138-187.

In this investigation Fabry assembled from both work performed at SCK-CEN and elsewhere a large dataset reflecting the embrittlement properties of the surveillance reference material used in both the American Yankee Rowe vessel and in the Belgian reactor BR-3 (Belgian Reactor 3). Data spanning a wide flux range were presented. In the plots the symbols indicate the neutron flux as being "low" or "high," with the division between these two categories being set at $1x10^{12}$ $n/cm^2/s$ because this flux defines the upper end of fluxes seen in power reactors. Additionally, the symbols indicate which datum are based on surveillance; all of these data are low flux.

Table G.6. Summary materials and irradiation condition studied in Fabry 96.

Short ID: Fabry 96 Category: Low and High Flux

Material	Product	Specification	Cu [wt-%]	Ni [wt-%]	P [wt-%]	Mn [wt-%]
Yankee & BR3 Surveillance Reference Material	Plate	ASTM A302B	0.2	0.18	0.012	1.36

Source	Reactor	Capsule Location	Irradiation Temperature [°F]	Flux [n/cm²/sec]	Notes
NUREG/CR-3295	PSF		550.4	2E+11 to 6E+12	See Hawthorne 85 for details, ASTM reference plate.
NUREG/CR-5493	UBR		554	8E+10, 6E+11, and 9E+12	
NRL-6616&6772	LITR		554	6E+12	
Surveillance	Yankee Rowe & BR-3	Surveillance	554	8E+10	

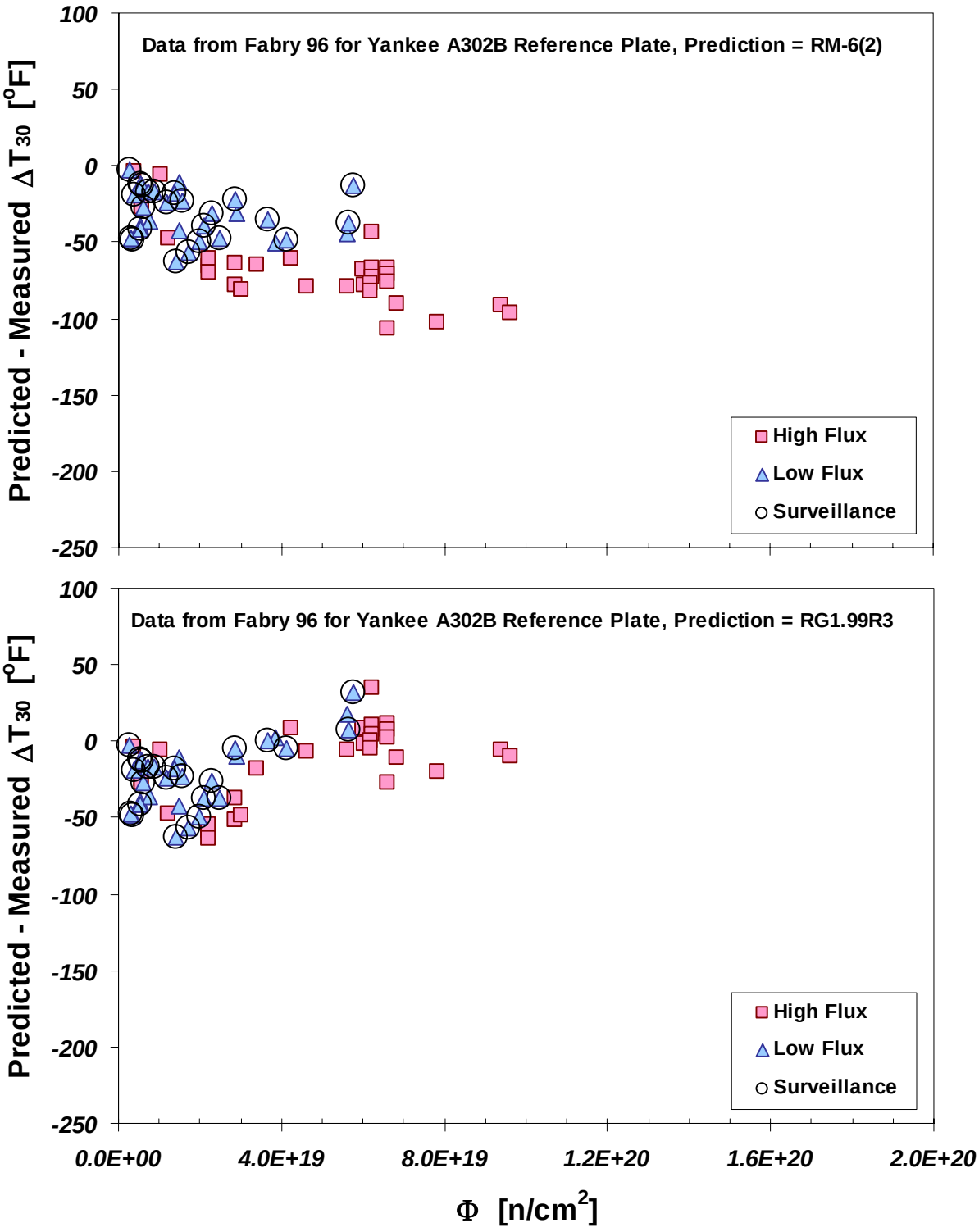

Figure G-18. Assessment of how well Fabry 96 data are predicted by (top) the ΔT_{30} model RM-6(2), which was calibrated only to US-LWR surveillance data, and by (bottom) the ΔT_{30} model recommended for use in Revision 3 of Regulatory Guide 1.99.

Citation: **Kussmaul 90**, Kussmaul, K., Föhl, J., and Weissenberg, T., "Investigation of Materials from a Decommissioned Reactor Pressure Vessel – A Contribution to the Understanding of Irradiation Embrittlement, *Effects of Radiation on Materials: 14th International Symposium, ASTM STP 1046*, N.H. Packin, R.E. Stoller, and A.S. Kumar, Eds., American Society for Testing and Materials, Philadelphia, 1990, pp. 80-104.

In this citation Kussmaul reports surveillance data for a weld and a forging in Gundremmingen Unit A. Figure G-19 compares the flux and fluence conditions reported by Kussmaul with those of the larger databases documented in the main body of this report.

Table G.7. Summary materials and irradiation condition studied in Kussmaul 90.

Short ID: Kussmaul 90 Category: Low Flux Only

Material	Product	Specification	Cu [wt-%]	Ni [wt-%]	P [wt-%]	Mn [wt-%]
Forging 7.1	Forging	DIN 20 NiMoCr 2 6	0.16	0.745	0.013	0.71
Weld W7	Weld	Sub Arc	0.25	0.2	0.009	1.33

Reactor	Capsule Location	Irradiation Temperature [°F]	Flux [n/cm²/sec]	Fluence [n/cm²]
Gundremmingen A	Surveillance	543	2.2E+10	2.9E+18
			8.6E+10	5.0E+18
			3.1E+11	1.8E+19
			1.7E+12	9.7E+19

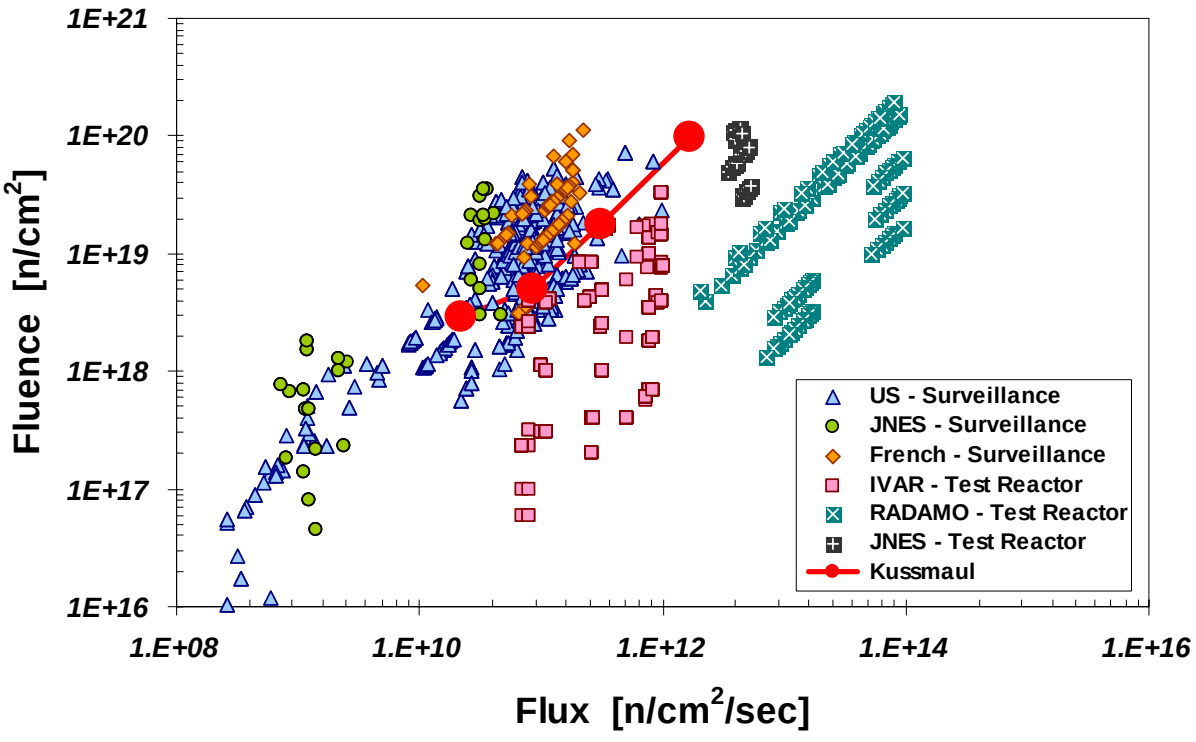

Figure G-19. Comparison of fluence and flux conditions reported by Kussmaul with the larger data sets documented in the main body of this report.

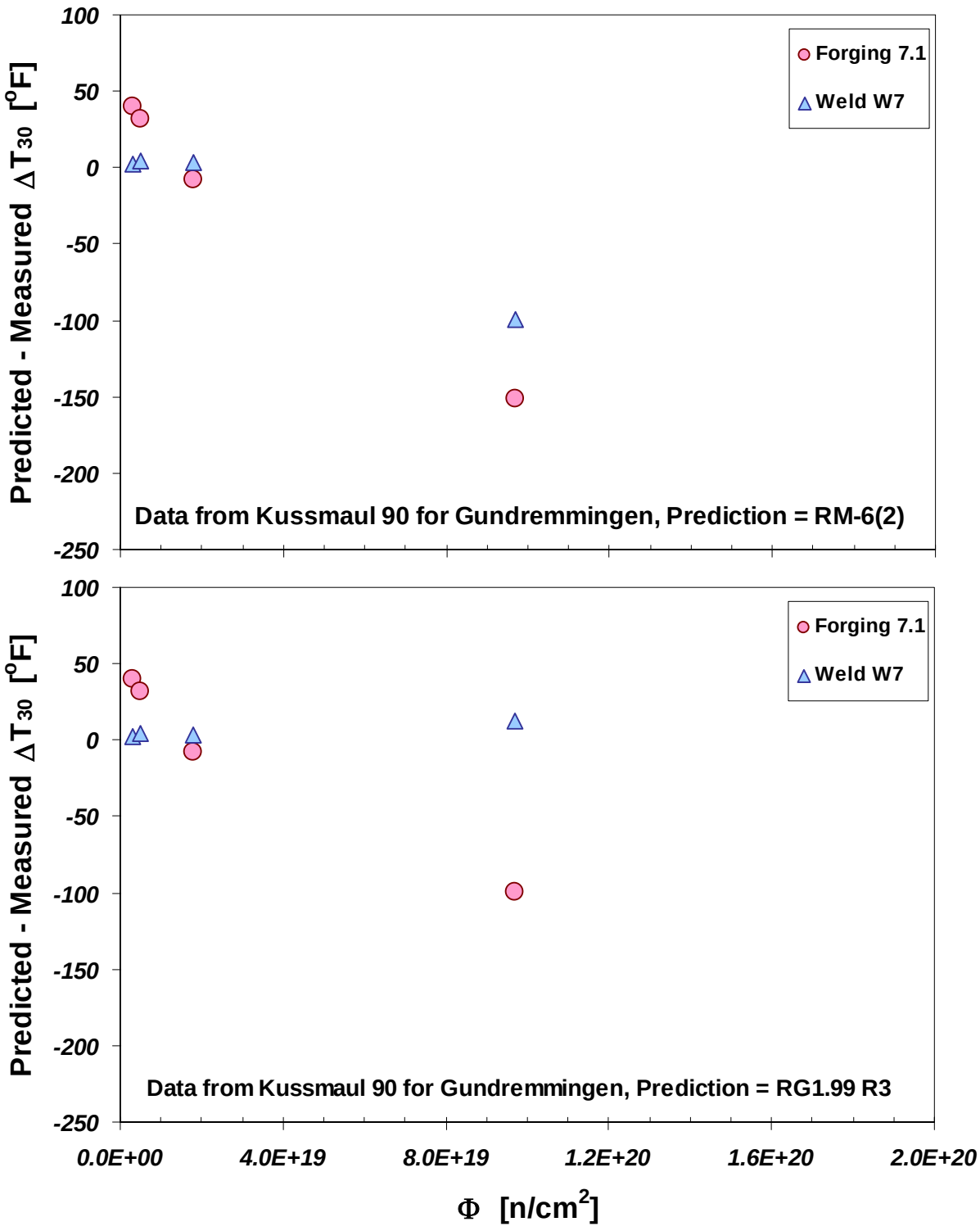

Figure G-20. Assessment of how well Kussmaul 90 data are predicted by (top) the ΔT_{30} model RM-6(2), which was calibrated only to US-LWR surveillance data, and by (bottom) the ΔT_{30} model recommended for use in Revision 3 of Regulatory Guide 1.99.

Citation: **Brillaud 01**, Brillaud, C., Grandjean, Y., and Saillet, S., "Vessel Investigation Program of 'CHOOZ A' PWR Reactor after Shutdown," *Effects of Radiation on Materials: 20th International Symposium, ASTM STP 1405*, S.T. Rosinski, M.L. Grossbeck, T.R. Allen, and A.S. Kumar, Eds., American Society for Testing and Materials, West Conshohcken Pennsylvania, 2001, pp. 28-41.

In this investigation Brillaud reports low flux data from both the Chooz-A surveillance program and from trepan samples that were removed from the vessel and tested after it was retired from operation in 1991. As documented in Table G.8, while the Chooz-A materials are similar to US RPV materials in terms of chemistry, the following two factors distinguish them from the US-LWR database:

- The French practice is to report Charpy V-notch transition temperatures at a 56J index energy, rather than at a 41J index energy, as is the American practice. No attempt has been made to correct for this difference, however it should be noted that 56J-indexed shift values will tend to be larger than 41J-indexed values due to upper shelf effects.
- Chooz-A ran at temperatures lower than both BWRs and PWRs in the United States, where the lowest temperature in the US-LWR database is ≈525 °F. It was recognized that the temperature function used in fitting the US-LWR data is not amenable to large extrapolations, and will over-estimate embrittlement for irradiation temperatures below its calibrated range. To enable comparison of the predictions of the RM-6(2) model with the Chooz-A data the matrix damage temperature factor was therefore set to 1.4 (based on the work of [Chaouadi 05]), rather than the 3.63 value predicted by the RM-6(2) formula.

Despite these dissimilarities, the Chooz-A data were viewed as being a valuable addition to our investigation of high fluence effects and, therefore, were retrained for analysis subject to the differences noted above. Figure G-21 compares the Brillaud 01 data for Chooz-A with the trend curve predictions. Also, Figure G-22 compares data reported earlier by Brillaud [Brillaud 92] for the entire French surveillance program. The [Brillaud 92] data are included here because (a) they feature high fluence data, and (b) the "Low Temp." forging data noted in Figure G-22 are a subset of the Chooz-A data reported in Figure G-21.

Table G.8. Summary materials and irradiation condition studied in Brillaud 01.

Short ID: Brillaud 01 Category: Low Flux Only

Material	Product	Specification	Cu [wt-%]	Ni [wt-%]	P [wt-%]	Mn [wt-%]
Shell C	Forging	ASTM A336	0.1	0.61	0.01	1.26
Shell B	Forging	ASTM A336	0.08	0.59	0.015	1.22

Reactor	Capsule Location	Irradiation Temperature [°F]	Flux [n/cm²/sec]	Notes
CHOOZ Unit A	Surveillance	491 from 1967 to 1975, 509 from 1975 to 1991	1.24E+11	
	Trepan at 1/4T thickness location		9.65E+10	Shell C, based on attenuation from surveillance location
			9.48E+10	Shell B, based on attenuation from surveillance location

Notes: Transition temperatures were reported at 56J rather than at 41J index energy.
Flux not reported in this citation, but was reported by [Brillaud 92] at the surveillance location.
Attenuation effect estimated using equation from Regulatory Guide 1.99 Revision 2.

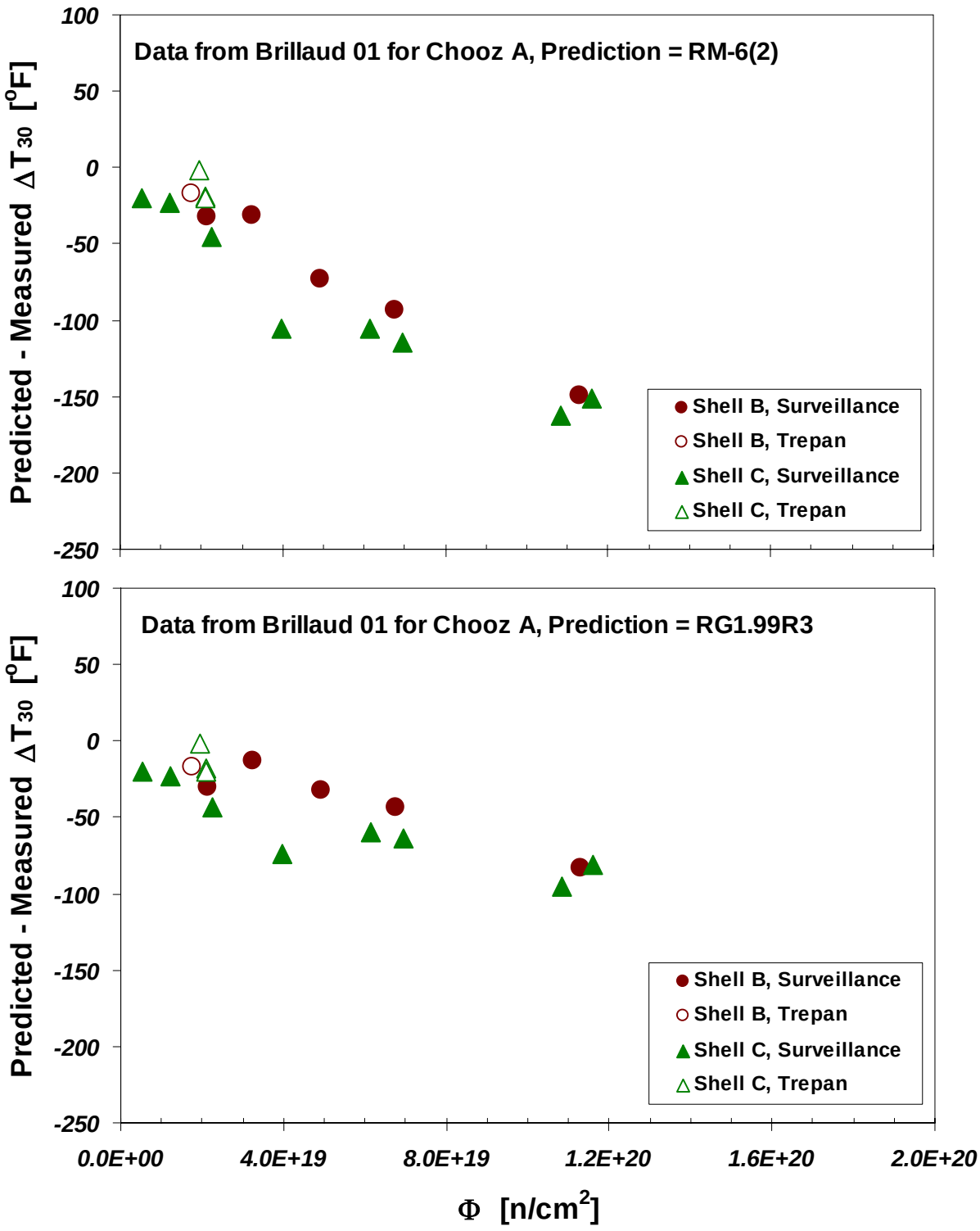

Figure G-21. Assessment of how well Brillaud 01 data are predicted by (top) the ΔT_{30} model RM-6(2), which was calibrated only to US-LWR surveillance data, and by (bottom) the ΔT_{30} model recommended for use in Revision 3 of Regulatory Guide 1.99.

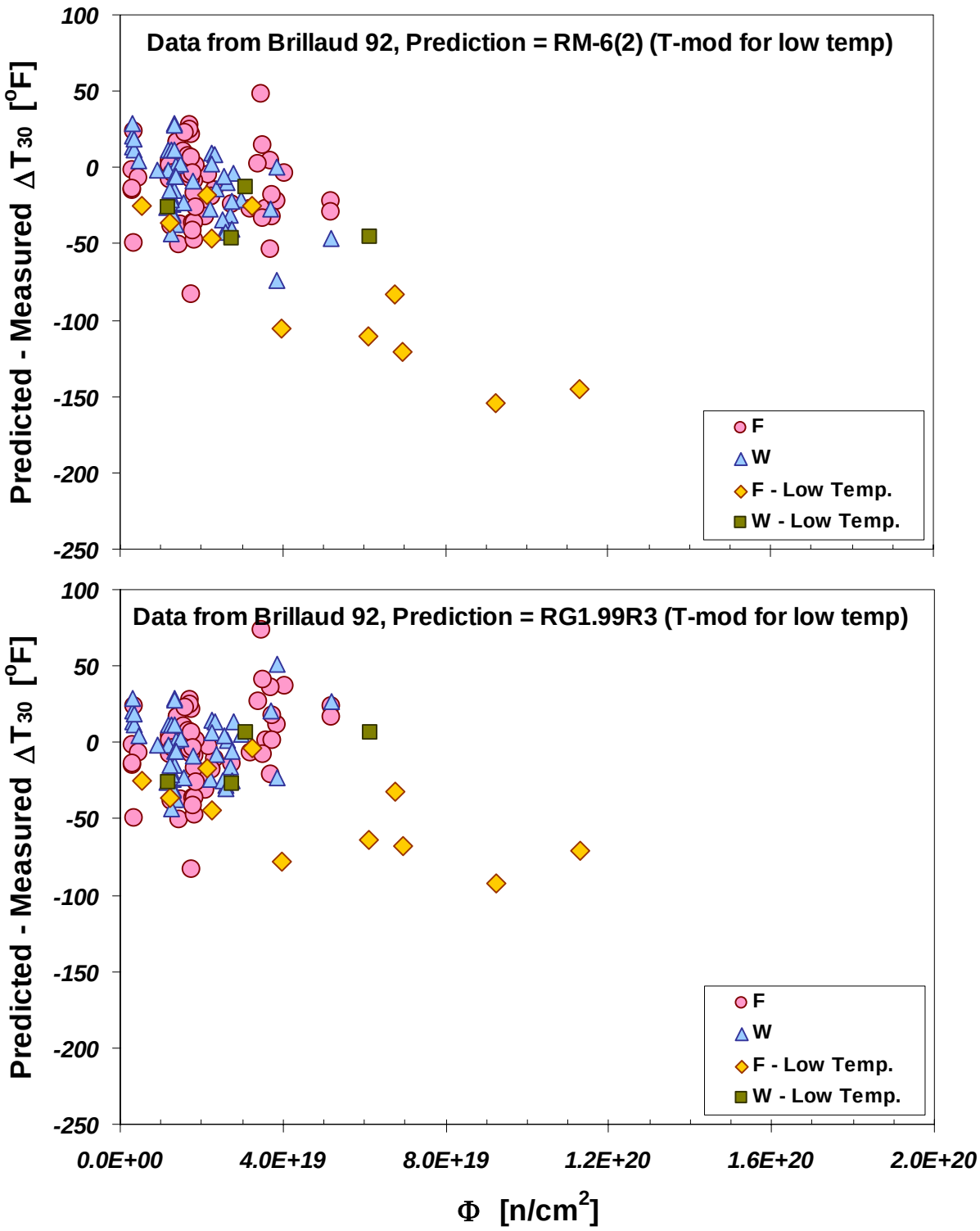

Figure G-22. Assessment of how well Brillaud 92 data for the overall French RPV surveillance program are predicted by (top) the ΔT_{30} model RM-6(2), which was calibrated only to US-LWR surveillance data, and by (bottom) the ΔT_{30} model recommended for use in Revision 3 of Regulatory Guide 1.99. The low temperature data shown in these plots are a subset of the Chooz-A data reported in Brillaud 01.

Citation: **Bellmann 90**, Bellmann, D., and Ahlf, J., "Comparison of Experimental 41J Shifts with the Predictions of German KTA 3203 and U.S. NRC Regulatory Guide 1.99," *Effects of Radiation on Materials: 14th International Symposium, ASTM STP 1046*, N.H. Packin, R.E. Stoller, and A.S. Kumar, Eds., American Society for Testing and Materials, Philadelphia, 1990, pp. 265-283.

In 1990 Bellmann reported the results of an extensive test reactor irradiation project conducted in Germany. One aim of that project was to collect data at high fluences in order to test the accuracy on extrapolation of various ETCs. On the basis of this information in Bellmann's conclusions he notes that "*Reg. Guide 1.99 Prop. Rev 2 is nonconservative in the high fluence range regardless of the copper of nickel content of the particular steel*."

Table G.9. Summary materials and irradiation condition studied in Bellman 90.

Short ID: Bellmann 90 Category: High Flux Only

Material	Product	Specification	Cu [wt-%]	Ni [wt-%]	P [wt-%]	Mn [wt-%]
GKSS-M	Forging	DIN 20 MnMoNi 5 5	0.022	0.46	0.007	1.29
GKSS-S	Weld	Sub Arc Weld	0.15	0.79	0.015	1.21
HSST03	Plate	ASTM A533B	0.12	0.56	0.011	1.26
IAEA-FF	Forging	ASTM A508 Cl. 3	0.07	0.69	0.009	1.37
IAEA-JF	Forging	ASTM A508 Cl. 3	0.06	0.76	0.009	1.35
IAEA-GW	Weld	Sub Arc Weld	0.05	0.93	0.015	1.48
KS01	Forging	DIN 22 NiMoCr 3 7	0.11	0.95	0.009	0.71
KS0ISG	Weld	Sub Arc Weld	0.42	1.23	0.017	1.64
KS02	Forging	DIN 22 NiMoCr 3 7	0.1	1.21	0.005	0.99
KS07B	Forging	DIN 22 NiMoCr 3 7	0.26	0.74	0.022	0.62
KS12	Forging	DIN 20 MnMoNi 5 5	0.17	0.63	0.015	1.48
KS15	Forging	DIN 20 MnMoNi 5 5	0.16	0.56	0.011	1.4
KS16C	Forging	DIN 22 NiMoCr 3 7	0.21	0.75	0.02	0.73
KS16D	Forging	DIN 22 NiMoCr 3 7	0.21	0.75	0.018	0.71
KS16E	Forging	DIN 22 NiMoCr 3 7	0.21	0.75	0.022	0.74
KS16G	Forging	DIN 22 NiMoCr 3 7	0.19	0.75	0.016	0.69
KS16H	Forging	DIN 22 NiMoCr 3 7	0.2	0.76	0.004	0.77
KS16K	Forging	DIN 22 NiMoCr 3 7	0.2	0.76	0.005	0.76
KS16M	Forging	DIN 22 NiMoCr 3 7	0.2	0.76	0.004	0.72
KS16S	Forging	DIN 22 NiMoCr 3 7	0.11	0.74	0.006	0.72

Reactor	Capsule Location	Irradiation Temperature [°F]	Flux [n/cm²/sec]	Notes
FRG-2	Reflector	554	0.2 to 3E+13	

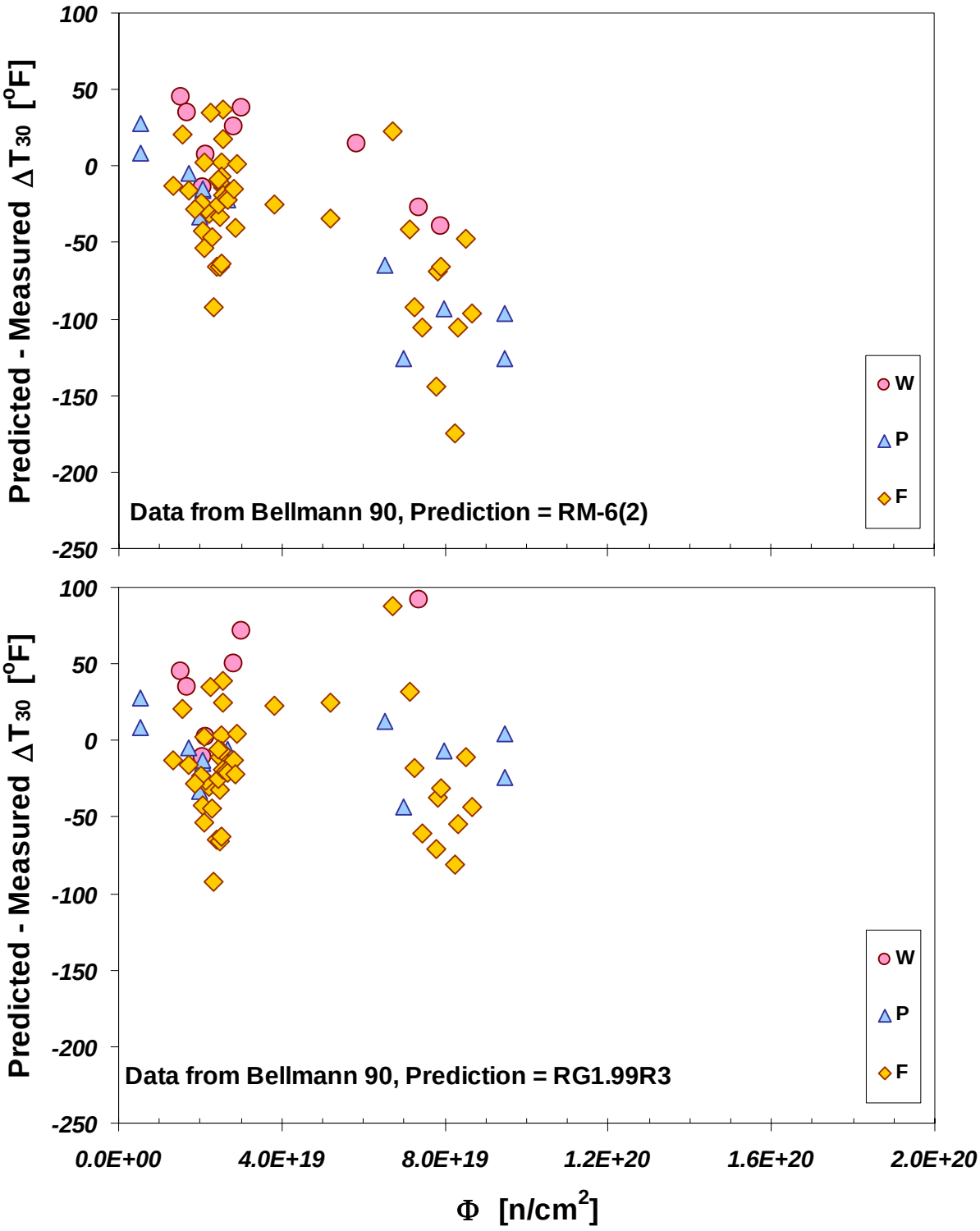

Figure G-23. Assessment of how well Bellman 90 data are predicted by (top) the ΔT_{30} model RM-6(2), which was calibrated only to US-LWR surveillance data, and by (bottom) the ΔT_{30} model recommended for use in Revision 3 of Regulatory Guide 1.99.

Citation: **Ishino 90**, Ishino S, Kawakami T, Hidaka T, and Satoh M., "The effect of chemical composition on irradiation embrittlement," *Nucl Eng Des* 1990(119): 139–48.

In 1990 Ishino reported a test reactor irradiation study for a variety of RPV materials. Note that, as expected, the one high nickel material studied (4B) is not well predicted by RM-6(2).

Table G.10. Summary materials and irradiation condition studied in Ishino 90.

Short ID: Ishino 1990 Category: High Flux Only

Material	Product	Specification	Cu [wt-%]	Ni [wt-%]	P [wt-%]	Mn [wt-%]
1B	Plate		0.06	0.58	0.008	1.46
2B	Plate		0.25	0.59	0.007	1.43
3B	Plate		0.06	0.57	0.018	1.44
4B	Plate		0.06	1.78	0.009	1.44
5B	Plate		0.23	0.61	0.018	1.41
1W	Weld		0.06	0.98	0.007	1.28
5W	Weld		0.25	1.06	0.019	1.3

Reactor	Capsule Location	Irradiation Temperature [^{o}F]	Flux [n/cm^{2}/sec]	Notes
JMTR	Not stated	554	1E+13	

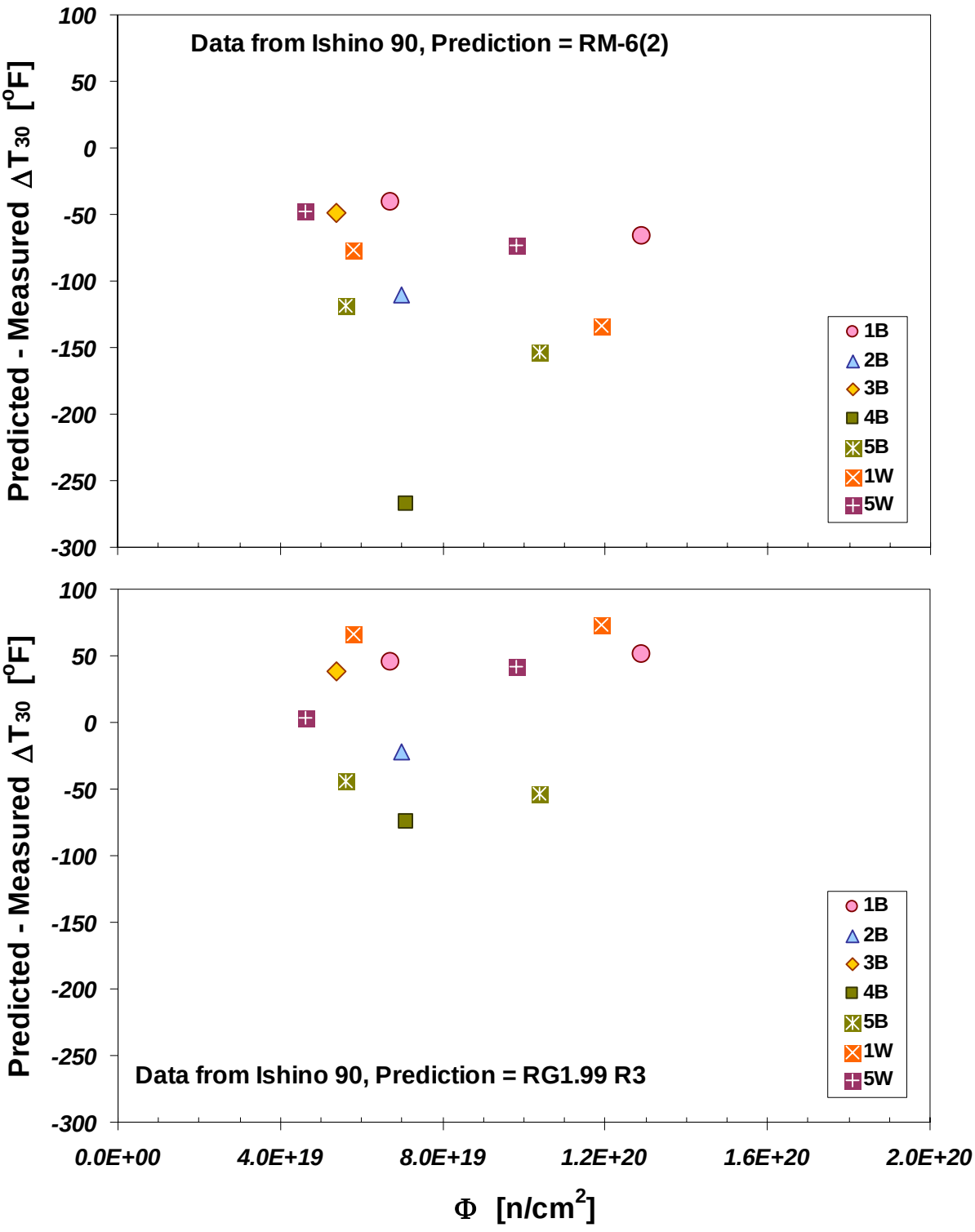

Figure G-24. Assessment of how well Ishino 90 data are predicted by (top) the ΔT_{30} model RM-6(2), which was calibrated only to US-LWR surveillance data, and by (bottom) the ΔT_{30} model recommended for use in Revision 3 of Regulatory Guide 1.99.

Citation: **Pachur 90**, Pachur, D., "Comparison of Drop-Weight and Instrumented Charpy Impact Test Results for Irradiated RPV," *Effects of Radiation on Materials: 16th International Symposium, ASTM STP 1175*, A.S. Kumar, D.S. Gelles, R.K. Nanstad, and E.A. Little, Eds., American Society for Testing and Materials, Philadelphia, 1993, pp. 195-210.

In 1990 Pachur reported a test reactor irradiation study for two RPV forgings.

Table G.11. Summary materials and irradiation condition studied in Pachur 93.

Short ID: Pachur 93 Category: High Flux Only

Material	Product	Specification	Cu [wt-%]	Ni [wt-%]	P [wt-%]	Mn [wt-%]
Forging A&B	Forging	DIN 20MnMoNi55	0.17	0.63	0.015	1.47

Reactor	Capsule Location	Irradiation Temperature [°F]	Flux [n/cm²/sec]	Notes
FRJ-1 (Light Water)	Not stated	550.4	3E+12	

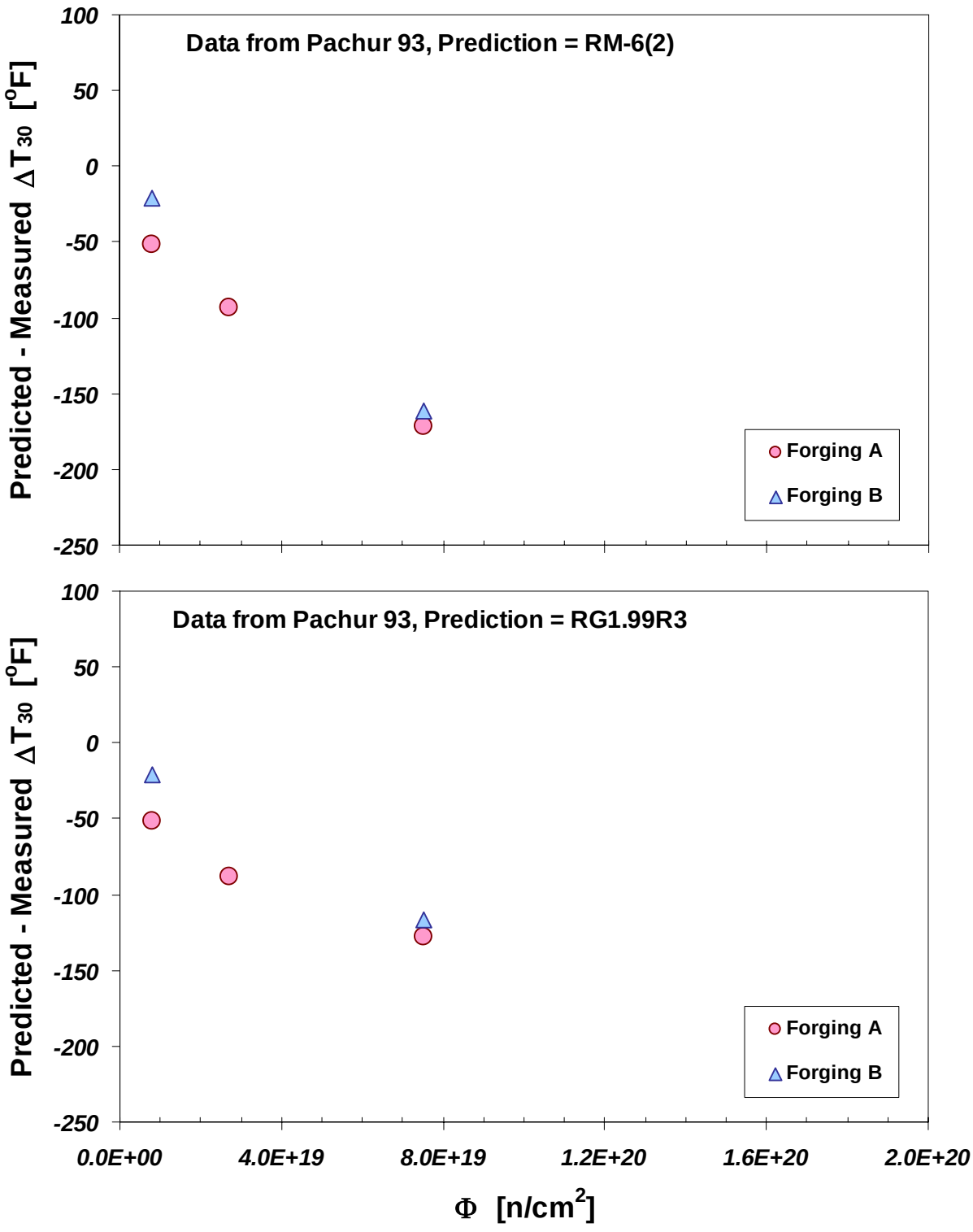

Figure G-25. Assessment of how well Pachur 93 data are predicted by (top) the ΔT_{30} model RM-6(2), which was calibrated only to US-LWR surveillance data, and by (bottom) the ΔT_{30} model recommended for use in Revision 3 of Regulatory Guide 1.99.

Citation: **Leitz 93**, Leitz, C., Klausnitzer, E.N., and Hofmann, G., "Annealing Experiments on Irradiated NiCrMo Weld Metal," *Effects of Radiation on Materials: 16th International Symposium, ASTM STP 1175*, A.S. Kumar, D.S. Gelles, R.K. Nanstad, and E.A. Little, Eds., American Society for Testing and Materials, Philadelphia, 1993, pp. 352-362.

In 1993 Leitz reported a test reactor irradiation study of a RPV weld.

Table G.12. Summary materials and irradiation condition studied in Leitz 93.

Short ID: Leitz 93 Category: High Flux Only

Material	Product	Specification	Cu [wt-%]	Ni [wt-%]	P [wt-%]	Mn [wt-%]
Weld A	Weld	Sub Arc	0.27	0.27	0.27	0.27

	Reactor	Capsule Location	Irradiation Temperature [°F]	Flux [n/cm^2/sec]	Notes
	15Mw BWR	Edge of core	541	2-4E+12	

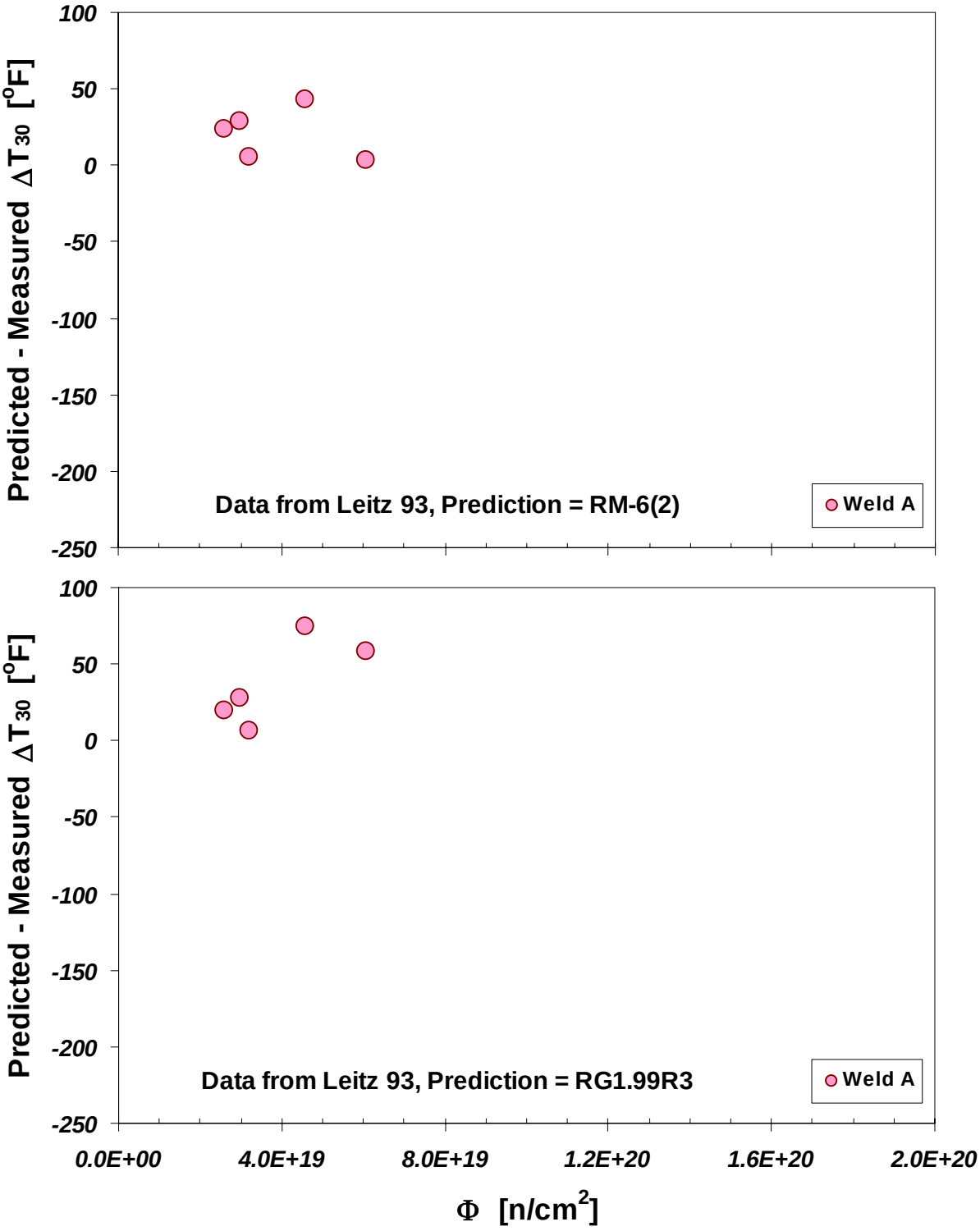

Figure G-26. Assessment of how well Leitz 93 data are predicted by (top) the ΔT_{30} model RM-6(2), which was calibrated only to US-LWR surveillance data, and by (bottom) the ΔT_{30} model recommended for use in Revision 3 of Regulatory Guide 1.99.

Citation: **Onizawa 01**, Onizawa, K., and Suzuki, M., "Comparison of Transition Temperature Shifts Between Static Fracture Toughness and Charpy-v Impact Properties Due to Irradiation and Post-Irradiation Annealing for Japanese A533B-1 Steels," *Effects of Radiation on Materials: 20th International Symposium, ASTM STP 1405*, S.T. Rosinski, M.L. Grossbeck, T.R. Allen, and A.S. Kumar, Eds., American Society for Testing and Materials, West Conshohcken Pennsylvania, 2001, pp. 79-96.

In 2001 Onizawa reported a test reactor irradiation study for four A533B plates.

Table G.13. Summary materials and irradiation condition studied in Onizawa 01.

Short ID: Onizawa 01 Category: High Flux Only

Material	Product	Specification	Cu [wt-%]	Ni [wt-%]	P [wt-%]	Mn [wt-%]
JRQ	Plate	ASTM A533B	0.14	0.84	0.017	1.42
Steel A	Plate	ASTM A533B	0.16	0.68	0.015	1.3
Steel B	Plate	ASTM A533B	0.04	0.65	0.004	1.43
Steel L	Plate	ASTM A533B	0.02	0.61	0.003	1.36

Reactor	Capsule Location	Irradiation Temperature [°F]	Flux [n/cm²/sec]	Notes
JMTR	Not stated	554	1.3-2E+13	

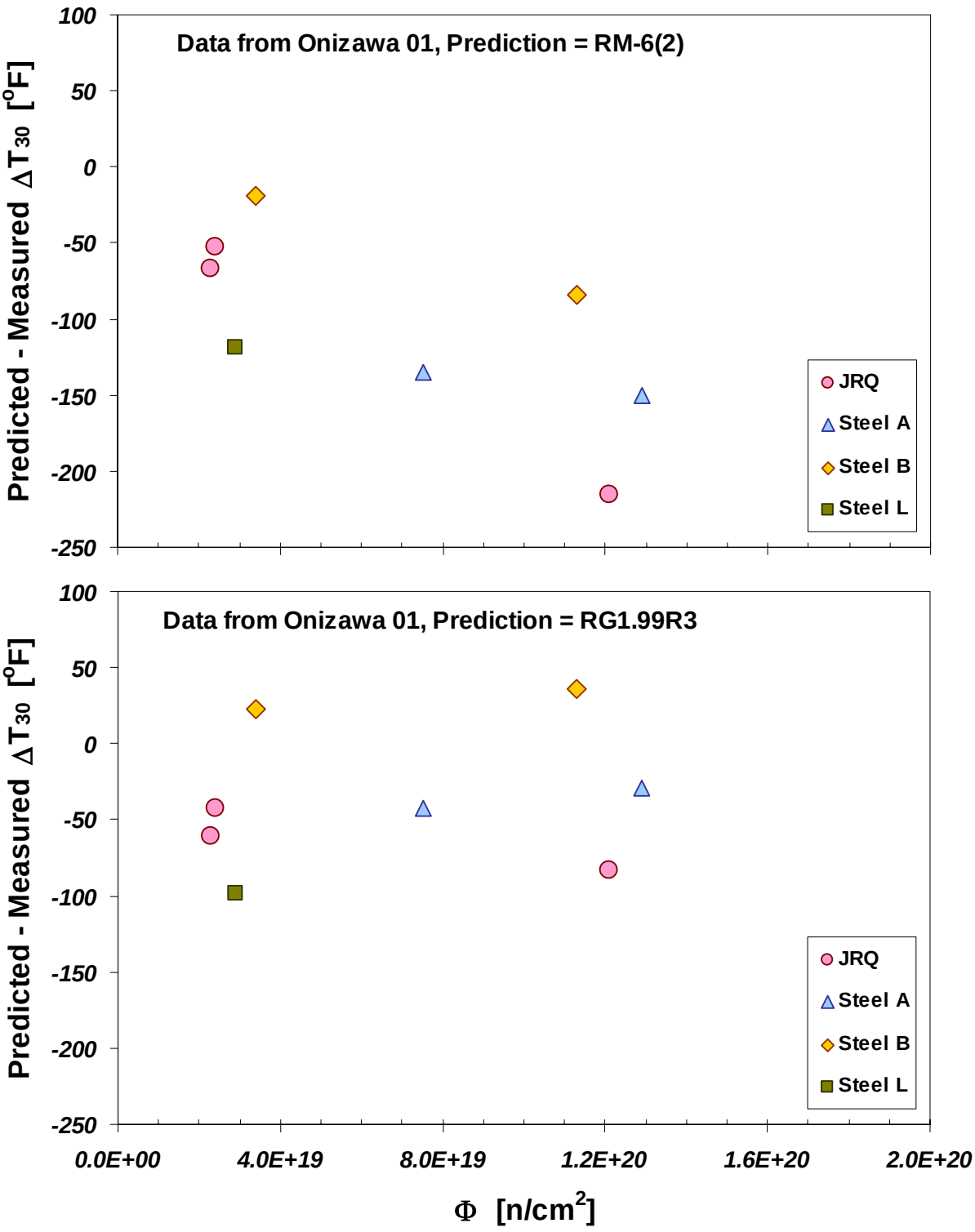

Figure G-27. Assessment of how well Onizawa 01 data are predicted by (top) the ΔT_{30} model RM-6(2), which was calibrated only to US-LWR surveillance data, and by (bottom) the ΔT_{30} model recommended for use in Revision 3 of Regulatory Guide 1.99.

Citation: **Lee 01**, Lee, B-S., Yang, W-J., Huh, M-Y., Chi, S-H., and Hong, J-H.,"Master Curve Characterization of Irradiation Embrittlement Using Standard and 1/3-Sized Precracked Charpy Specimens," *Effects of Radiation on Materials: 20th International Symposium, ASTM STP 1405*, S.T. Rosinski, M.L. Grossbeck, T.R. Allen, and A.S. Kumar, Eds., American Society for Testing and Materials, West Conshohcken Pennsylvania, 2001, pp. 55-67.

In 2001 Lee reported a test reactor irradiation study of two RPV materials.

Table G.14. Summary materials and irradiation condition studied in Lee 01.

Short ID: Lee 01 Category: High Flux Only

Material	Product	Specification	Cu [wt-%]	Ni [wt-%]	P [wt-%]	Mn [wt-%]
JRQ	Plate	ASTM A533B	0.14	0.84	0.017	1.42
SKA-1	Forging	ASTM A508 Cl.3	0.03	0.92	0.007	1.36

Reactor	Capsule Location	Irradiation Temperature [^{o}F]	Flux [n/cm^{2}/sec]	Notes
LVR-15	Not stated	550	Not stated	

Note: A flux of 1.0E+13 was assumed in evaluating the embrittlement trend curve predictions.

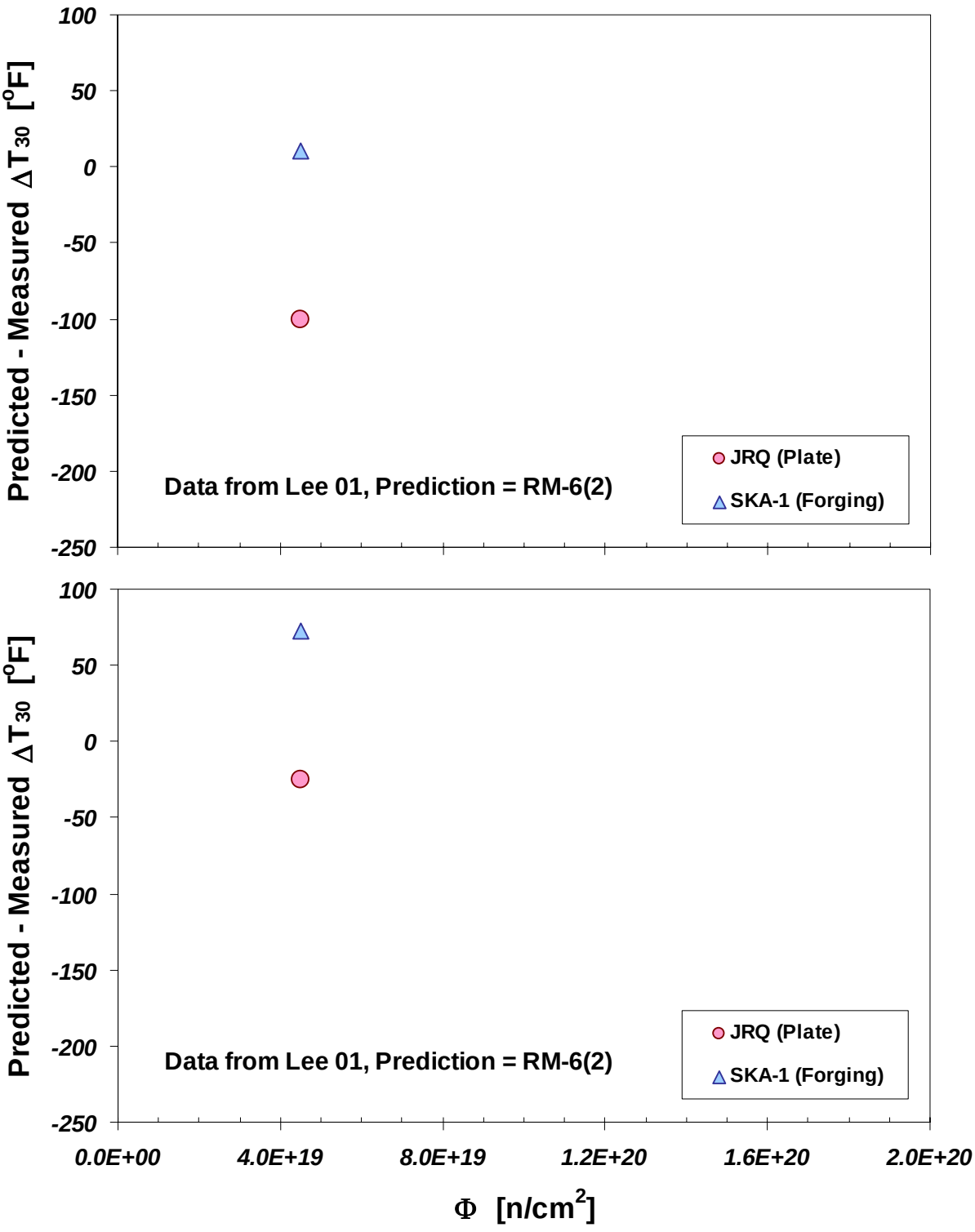

Figure G-28. Assessment of how well Lee 01 data are predicted by (top) the ΔT_{30} model RM-6(2), which was calibrated only to US-LWR surveillance data, and by (bottom) the ΔT_{30} model recommended for use in Revision 3 of Regulatory Guide 1.99.

Citation: **Nanstad 04**, Nanstad, R.K., et al., "Fracture Toughness, Thermo-Electric Power, and Atom Probe Investigations of JRQ Steel in I, IA, IAR, and IARA Conditions," *Effects of Radiation on Materials: 22nd International Symposium, ASTM STP 1475*, T.R. Allen, R.G. Lott, J.T. Busby, and A.S. Kumar, Eds., American Society for Testing and Materials, West Conshohcken Pennsylvania, 2006, pp. 195-211.

In 2004 Nanstad reported a test reactor irradiation study for the international reference material JRQ.

Table G.15. Summary materials and irradiation condition studied in Nanstad 04.

Short ID: Nanstad 04 Category: High Flux Only

Material	Product	Specification	Cu [wt-%]	Ni [wt-%]	P [wt-%]	Mn [wt-%]
JRQ	Plate	ASTM A533B	0.14	0.84	0.017	1.42

Reactor	Capsule Location	Irradiation Temperature [°F]	Flux [n/cm^2/sec]	Notes
SAPHIR	Not stated	554	5E+12	

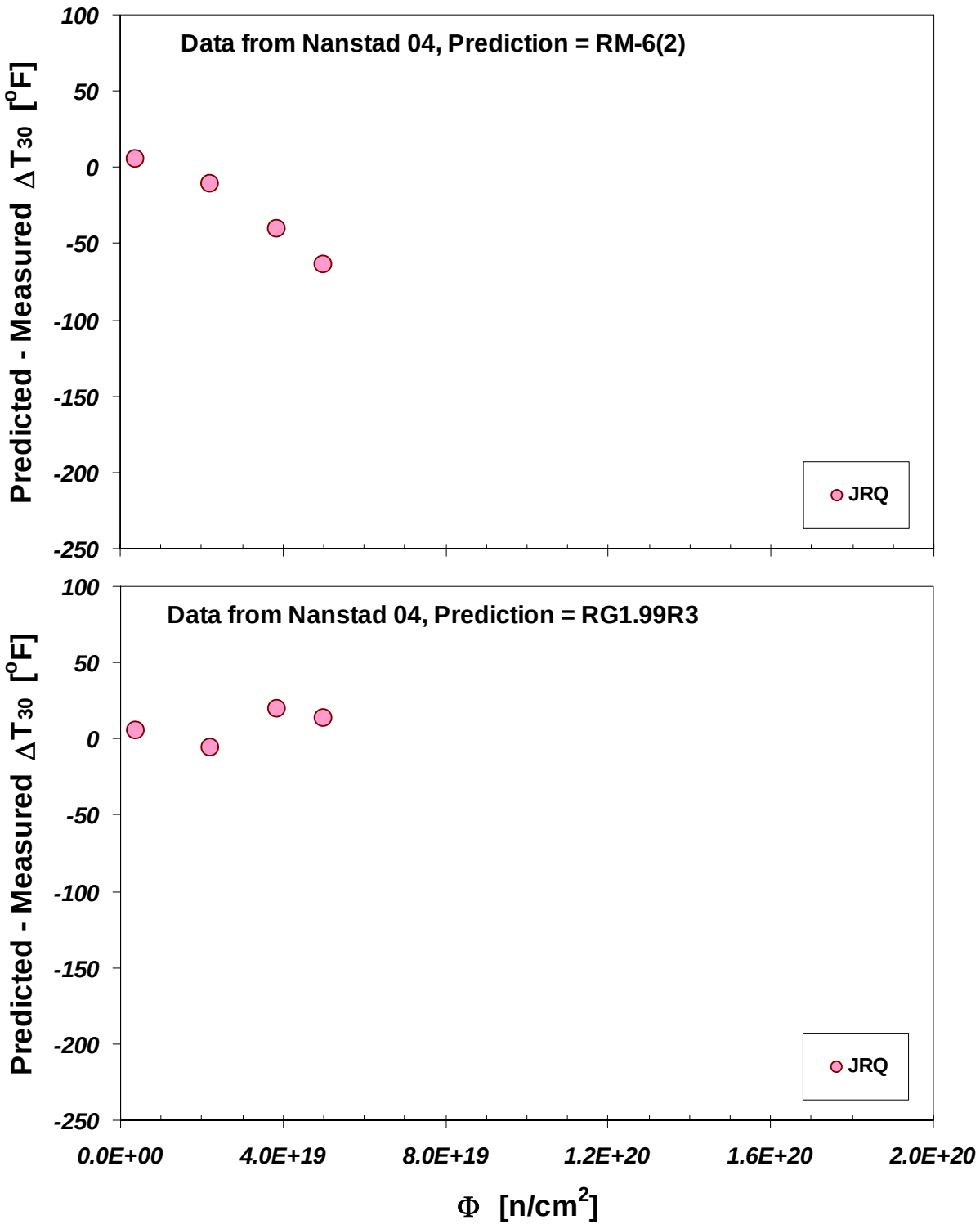

Figure G-29. Assessment of how well Nanstad 04 data are predicted by (top) the ΔT_{30} model RM-6(2), which was calibrated only to US-LWR surveillance data, and by (bottom) the ΔT_{30} model recommended for use in Revision 3 of Regulatory Guide 1.99.

Citation: **Gérard 06**, Gérard, R., E. Lucon, M.Scibetta, R.Chaouadi, and E. Van Walle, "Reactor Pressure Vessel Steels Embrittlement at Very High Neutron Doses," *Fontevraud 6th International Symposium on Contribution of Material Investigations to Improve Safety and Performance of LWRs*, September 18–22, 2006, Fontevraud-L'Abbaye, France.

In 2006 Gérard reported a comparison of test and power reactor irradiations for both RPV welds and forgings. In this study irradiation damage was quantified by yield strength change; yield strength change is converted to transition temperature shift in Figure G-30 for consistency with the bulk of the data reported in this Appendix. It should be noted that because the same conversion constants are applied to both Gérard's data and to the prediction equations the trends shown on the graphs will be the same regardless of if yield strength change or transition temperature shift is used.

The 2006 Gérard data were reported in the main body of this report, and are repeated here for completeness.

Table G.16. Summary materials and irradiation condition studied in Gérard 06.

Short ID: Gérard 06 Category: Low and High Flux

Material	Product	Specification	Cu [wt-%]	Ni [wt-%]	P [wt-%]	Mn [wt-%]
Forging A1, A2, B1, B2	Forging	Materials are from operating Belgian PWRs, Spec not stated.	0.04 to 0.05	0.75 to 0.77	0.006 to 0.008	1.39 to 1.46
			0.043	0.76	0.007	1.42
Weld	Weld		0.065	0.8	0.015	1.11

Reactor	Capsule Location	Irradiation Temperature [°F]	Flux [n/cm²/sec]	Notes
PWR	Surveillance on thermal shield	572	1.4E+11	
BR-2	Not stated	572	7.0E+13	

Note: Results reported for four forgings of nearly identical chemistry. Average composition values used for ΔT_{30} calc.

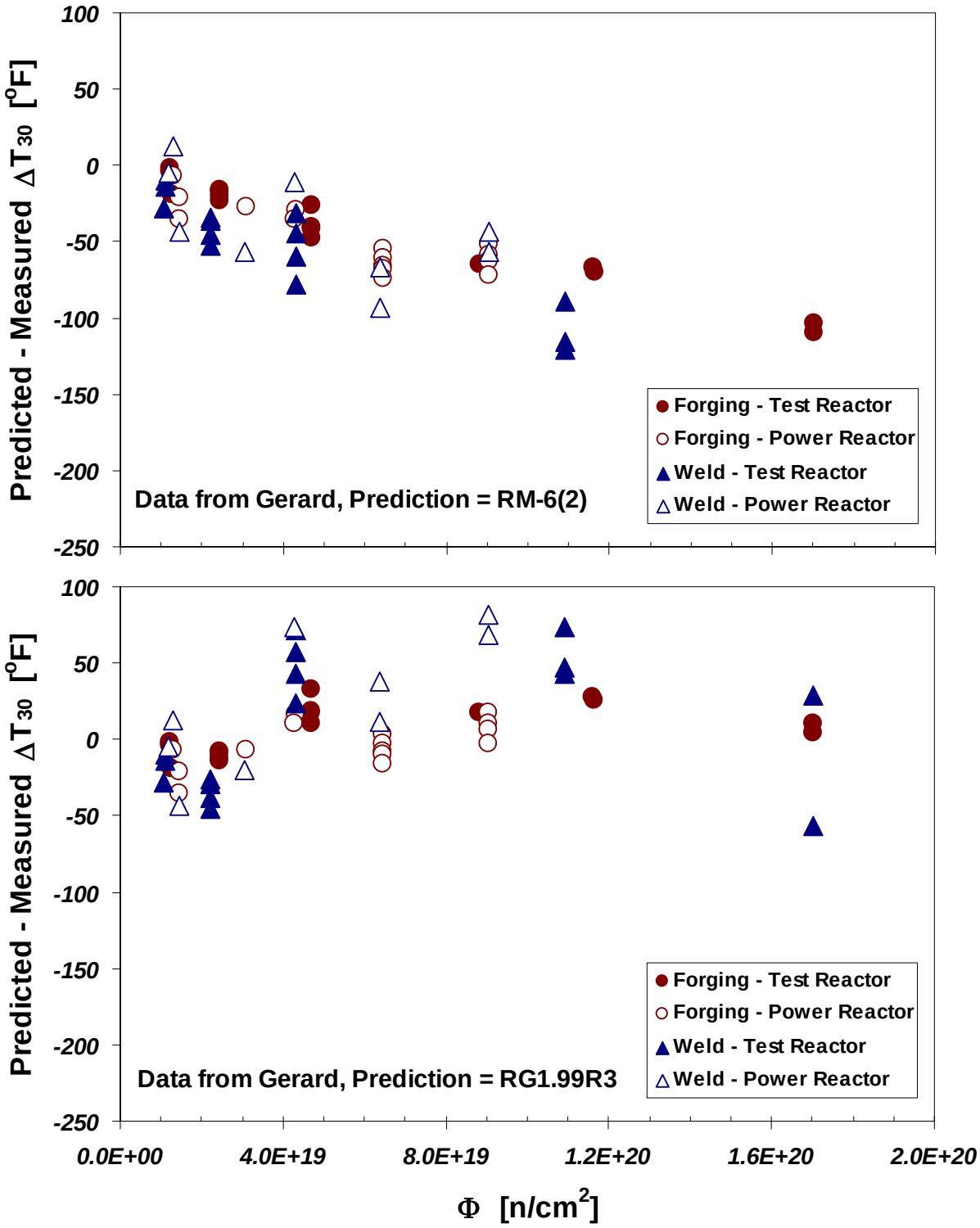

Figure G-30. Assessment of how well Gérard 06 data are predicted by (top) the ΔT_{30} model RM-6(2), which was calibrated only to US-LWR surveillance data, and by (bottom) the ΔT_{30} model recommended for use in Revision 3 of Regulatory Guide 1.99.

Citation: **RADAMO 05**, R. Chaouadi, "An Engineering Radiation Hardening Model for RPV Materials," SCK/CEN Report R-4235, September 2005.

In 2005 Chaouadi reported the results of a comprehensive test reactor irradiation study called RADAMO. In this study irradiation damage was quantified by yield strength change; yield strength change is converted to transition temperature shift in Figure G-31 for consistency with the bulk of the data reported in this Appendix. It should be noted that because the same conversion constants are applied to both Gérard's data and to the prediction equations the trends shown on the graphs will be the same regardless of if yield strength change or transition temperature shift is used.

The RADAMO database also included test reactor irradiations of four VVER steels. These data have been excluded from this presentation.

The 2005 RADAMO data were reported in the main body of this report, and are repeated here for completeness.

Table G.17. Summary materials and irradiation condition studied in RADAMO 05.

Short ID: RADAMO-05 Category: High Flux Only

Material	Product	Specification	Cu [wt-%]	Ni [wt-%]	P [wt-%]	Mn [wt-%]
JRQ	Plate	ASTM A533B	0.14	0.84	0.017	1.42
HSST-03	Plate	ASTM A533B	0.12	0.62	0.011	1.36
73W	Weld	Sub Arc	0.31	0.6	0.005	1.56
18MND5 BM	Plate	French 18MND5	0.13	0.64	0.008	1.55
18MND5 weld	Weld	Sub Arc	0.12	1.01	0.021	1.3
A508 Cl.3 BM	Forging	ASTM A508 Cl. 3	0.05	0.75	0.008	1.43
A508 Cl.3 weld	Weld	Sub Arc	0.07	0.83	0.015	1.57
20MnMoNi55	Forging	DIN 20MnMoNi55	0.11	0.8	0.007	1.29
72W	Weld	Sub Arc	0.23	0.6	0.006	1.6
16MND5	Forging	French 16MND5	0.065	0.69	0.013	1.37

Reactor	Capsule Location	Irradiation Temperature [^{o}F]	Flux [n/cm^{2}/sec]	Notes
BR-2	Castillo Loop, Channels K49 and D180	509 and 572	2E+12 to 9.6E+13	

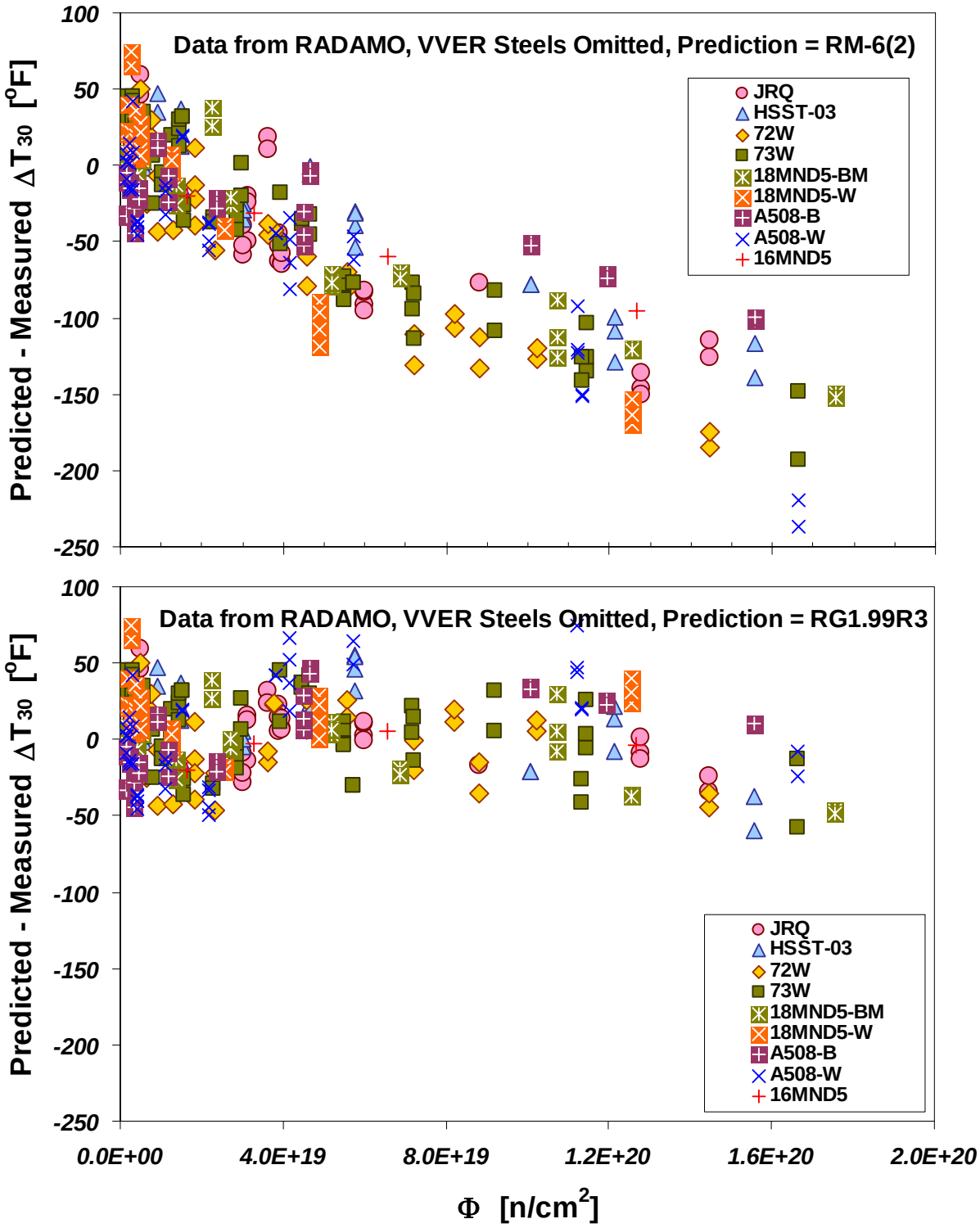

Figure G-31. Assessment of how well RADAMO 05 data are predicted by (top) the ΔT_{30} model RM-6(2), which was calibrated only to US-LWR surveillance data, and by (bottom) the ΔT_{30} model recommended for use in Revision 3 of Regulatory Guide 1.99.

Citation: **JNES 07**, JNES-SS-0707, "Accuracy and Reliability of the Revised Transition Temperature Shift Prediction in the Japan Electrical Association Code, to be published.

In 2007 JNES reported the results of a large number of power and test reactor irradiation studies as part of a project aimed at updating the Japanese regulatory practice on embrittlement prediction. Figure G-32 shows the distribution of copper and nickel contents in these databases.

The 2007 JNES data were reported in the main body of this report, and are repeated here for completeness.

Table G.18. Summary materials and irradiation condition studied in JNES 07.

Short ID: JNES-07 Category: High Flux Only

Material	Product	Specification	Cu [wt-%]	Ni [wt-%]	P [wt-%]	Mn [wt-%]
Plates Irrad in Power Reactors	Plate	Not stated. All typical of early PWR and BWR construction in Japan	0.09 - 0.24	0.54 - 0.61	0.01 - 0.02	Not stated
Welds Irrad in Power Reactors	Weld		0.06 - 0.19	0.66 - 1.08	0.01 - 0.015	Not stated
Plates Irrad in Test Reactors	Plate		0.04 - 0.21	0.59 - 0.92	0.005 - 0.017	Not stated
Welds Irrad in Test Reactors	Weld		0.02 - 0.2	0.84 - 0.88	0.008 - 0.016	Not stated

Reactor	Capsule Location	Irradiation Temperature [°F]	Flux [n/cm²/sec]	Notes
Power	Surveillance	554	7E+08 to 5E+10	
Test	Not stated	554	3.8 to 5.1E+12	

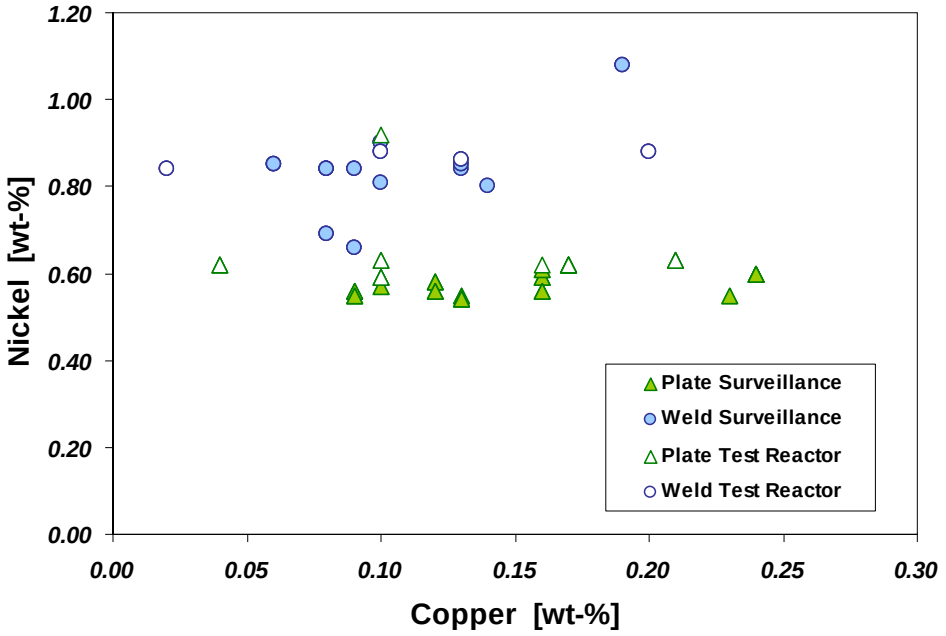

Figure G-32. Distribution of copper and nickel in the JNES databases.

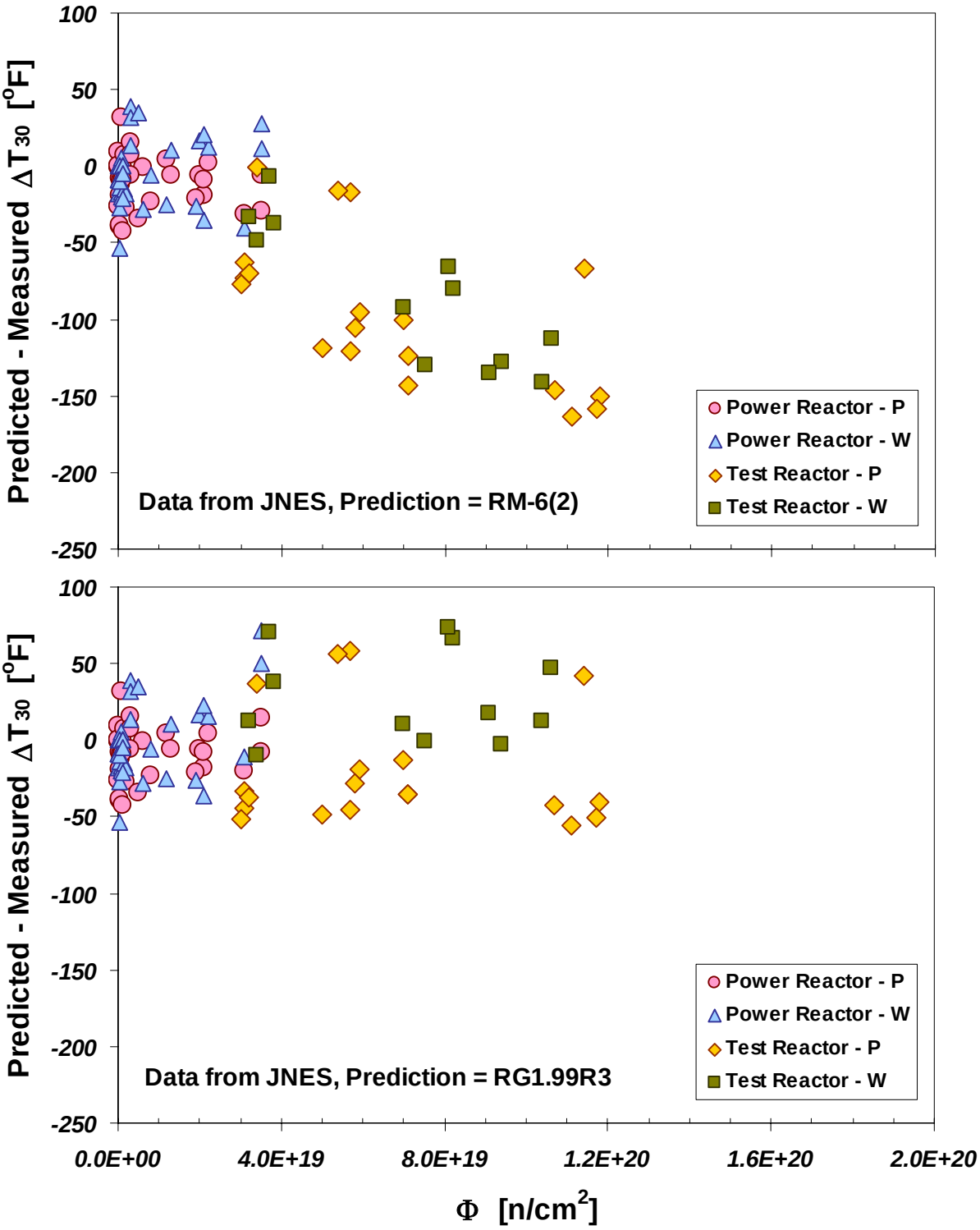

Figure G-33. Assessment of how well JNES 07 data are predicted by (top) the ΔT_{30} model RM-6(2), which was calibrated only to US-LWR surveillance data, and by (bottom) the ΔT_{30} model recommended for use in Revision 3 of Regulatory Guide 1.99.